

**PCT**WORLD INTELLECTUAL PROPERTY ORGANIZATION  
International Bureau

## INTERNATIONAL APPLICATION PUBLISHED UNDER THE PATENT COOPERATION TREATY (PCT)

<b>(51) International Patent Classification <sup>6</sup>:</b> <b>G01N 33/533</b>	<b>A1</b>	<b>(11) International Publication Number:</b> <b>WO 99/36779</b> <b>(43) International Publication Date:</b> 22 July 1999 (22.07.99)
<b>(21) International Application Number:</b> PCT/US99/00774 <b>(22) International Filing Date:</b> 14 January 1999 (14.01.99)  <b>(30) Priority Data:</b> 09/007,167 14 January 1998 (14.01.98) US  <b>(71)(72) Applicant and Inventor:</b> LAKOWICZ, Joseph, R. [US/US]; 10037 Fox Den Road, Ellicott City, MD 21042 (US).  <b>(72) Inventors:</b> CASTELLANO, Felix; Apartment 401, 7660 Woodpark Lane, Columbia, MD 21046 (US). MURTAZA, Zakir; 900 South Paca Street, Baltimore, MD 21230 (US).  <b>(74) Agents:</b> REPPER, George, R. et al.; Rothwell, Figg, Ernst & Kurz, Suite 701 East, Columbia Square, 555 13th Street N.W., Washington, DC 20004 (US).		<b>(81) Designated States:</b> CA, JP, European patent (AT, BE, CH, CY, DE, DK, ES, FI, FR, GB, GR, IE, IT, LU, MC, NL, PT, SE).  <b>Published</b> <i>With international search report. Before the expiration of the time limit for amending the claims and to be republished in the event of the receipt of amendments.</i>
<b>(54) Title:</b> METHOD OF CONDUCTING AN ASSAY OF A SAMPLE CONTAINING AN ANALYTE OF INTEREST  <b>(57) Abstract</b>  In accordance with the present invention, a method of conducting an assay of a sample containing an analyte of interest includes the step of forming a mixture so as to bring a metal-ligand complex into interactive proximity with the sample containing the analyte of interest. The mixture is irradiated with electromagnetic light energy so as to cause emission of light indicative of the analyte of interest. The emitted light is measured, and the measurement of the emitted light is utilized to measure the analyte of interest. The metal-ligand complex can be [Re(bcp)(CO) <sub>3</sub> (4-COOHPy)] <sup>+</sup> , [Os(phen) <sub>2</sub> (aphen)] <sup>2+</sup> , [Os(tpy)(triphos)] <sup>2+</sup> , [Os(tppz) <sub>2</sub> ] <sup>2+</sup> , and [Os(tppy) <sub>2</sub> ] <sup>2+</sup> , or the like. Also, the present invention is directed to a metal-ligand complex of the formula [Re(bcp)(CO) <sub>3</sub> (4-COOHPy)] <sup>+</sup> .		

**FOR THE PURPOSES OF INFORMATION ONLY**

Codes used to identify States party to the PCT on the front pages of pamphlets publishing international applications under the PCT.

AL	Albania	ES	Spain	LS	Lesotho	SI	Slovenia
AM	Armenia	FI	Finland	LT	Lithuania	SK	Slovakia
AT	Austria	FR	France	LU	Luxembourg	SN	Senegal
AU	Australia	GA	Gabon	LV	Latvia	SZ	Swaziland
AZ	Azerbaijan	GB	United Kingdom	MC	Monaco	TD	Chad
BA	Bosnia and Herzegovina	GE	Georgia	MD	Republic of Moldova	TG	Togo
BB	Barbados	GH	Ghana	MG	Madagascar	TJ	Tajikistan
BE	Belgium	GN	Guinea	MK	The former Yugoslav Republic of Macedonia	TM	Turkmenistan
BF	Burkina Faso	GR	Greece	ML	Mali	TR	Turkey
BG	Bulgaria	HU	Hungary	MN	Mongolia	TT	Trinidad and Tobago
BJ	Benin	IE	Ireland	MR	Mauritania	UA	Ukraine
BR	Brazil	IL	Israel	MW	Malawi	UG	Uganda
BY	Belarus	IS	Iceland	MX	Mexico	US	United States of America
CA	Canada	IT	Italy	NE	Niger	UZ	Uzbekistan
CF	Central African Republic	JP	Japan	NL	Netherlands	VN	Viet Nam
CG	Congo	KE	Kenya	NO	Norway	YU	Yugoslavia
CH	Switzerland	KG	Kyrgyzstan	NZ	New Zealand	ZW	Zimbabwe
CI	Côte d'Ivoire	KP	Democratic People's Republic of Korea	PL	Poland		
CM	Cameroon	KR	Republic of Korea	PT	Portugal		
CN	China	KZ	Kazakhstan	RO	Romania		
CU	Cuba	LC	Saint Lucia	RU	Russian Federation		
CZ	Czech Republic	LI	Liechtenstein	SD	Sudan		
DE	Germany	LK	Sri Lanka	SE	Sweden		
DK	Denmark	LR	Liberia	SG	Singapore		
EE	Estonia						

**METHOD OF CONDUCTING AN ASSAY OF A  
SAMPLE CONTAINING AN ANALYTE OF INTEREST**

BACKGROUND OF THE INVENTION

Field of the Invention

5           The present invention is in the field of conducting an assay of a sample containing an analyte of interest.

Description of the Background Art

10           In recent years there has been increased interest in the synthesis, characterization and application of metal-ligand complexes in biomolecule research. In addition to their use as photosensitizers, metal-ligand complexes have been used as luminescence probes in polymers. For instance, metal-containing intercalators  
15           such as square-planar platinum(II) complexes containing aromatic terpyridine or phenanthroline ligands have been used in probing DNA structure and the intercalation process itself. The reagent methidiumpropyl-Fe(II) EDTA, which contains a redox-  
20           active metal center tethered to an organic intercalator, has been applied in "footprinting" experiments to determine the sequence specificity of small drugs bound to DNA. Ru(II) and Os(II) transition metal compounds have been used to probe DNA structure  
25           and study long-range electron transfer.

          More recent studies have shown that ruthenium (Ru(II)), rhenium (Re(I)) and osmium (Os(II)) metal-ligand complexes display high anisotropy in the absence of rotational diffusion. Importantly, metal ligand

complexes display luminescence decay times ranging from 100 ns to 100  $\mu$ s. Consequently, these probes extend the observable timescale of anisotropy decay measurements by orders of magnitude compared with that observable with routinely used organic fluorophores. As a result of this, metal-ligand complexes have been used to probe the microsecond dynamics of DNA. In addition, time-resolved anisotropy measurements of proteins can be extended to the microsecond timescale using metal-ligand complexes. Intensity and anisotropy decays of Ru(II) metal-ligand complexes when covalently linked to human serum albumin, concanavalin A, human immunoglobulin G and ferritin demonstrated that this class of probes could be used to measure rotational motions from 10 ns to 1.5  $\mu$ s, which so far has been inaccessible using the classical organic fluorophores. Fluorescence polarization immunoassays using metal-ligand complexes covalently bound to human serum albumin (as the antigen) demonstrated the potential use of metal-ligand complexes in fluorescence polarization immunoassays of high-molecular-weight analytes.

Fluorescence polarization (FP) was first theoretically described by Perrin in 1926, which was subsequently expanded and measured by Weber. Dandliker and co-workers adapted FP for use in analytical biochemistry including antigen (Ag) - antibody (Ab) interactions, and hormone-receptor interactions. Since establishment of the theory and method by Dandliker, the use of FPI's (fluorescence polarization immunoassays) for the quantitative and qualitative measurement of various types of molecules and bioconjugates has been reported. These include therapeutic drug monitoring, determination of hormones, drugs of abuse, proteins and peptides, proteases and

inhibitors, as well as DNA binding interactions. In fact, FPI technology is presently in widespread commercial use in several instruments.

5 A serious limitation of present immunoassays is that they are limited to low molecular weight antigens. This limitation is a result of the use of fluorophores, such as fluorescein, which display lifetimes near 4 ns. A FPI requires that emission from the unbound labeled antigen be depolarized, so that an increase in  
10 polarization may be observed upon antigen binding to antibody. For depolarization to occur, the antigen must display a rotational correlation time much shorter than the lifetime of the probe (in the case of fluorescein, less than 4 ns) which limits the dynamic  
15 range of the FPI to antigens with low molecular weights (Figure 16). Some long lifetime fluorophores, such as chelates of  $\text{Eu}^{3+}$  and  $\text{Tb}^{3+}$  have been used in time-resolved immunoassays, but they do not display polarized emission and are thus not useful in FPI's.

20 More recent studies have shown that  $[\text{Ru}(\text{bpy})_2(\text{dcb})]^{2+}$ , where bpy is 2,2'-bipyridine and dcb is 4,4'-dicarboxylic acid-2,2'-bipyridine, displays high polarization in the absence of rotational diffusion ( $\sim 0.25$ ), as well as a long lifetime ( $\sim 400$   
25 ns). The experimental results demonstrated that the steady-state polarization of  $[\text{Ru}(\text{bpy})_2(\text{dcb})]^{2+}$  labeled to HSA was sensitive to the binding of anti-HSA, which resulted in a 200% increase in polarization. Another metal-ligand complex,  $[\text{Os}(\text{bpy})_2(\text{dcb})]^{2+}$ , was also used  
30 in a FPI to detect a high molecular weight bioconjugate using red excitation and emission wavelengths.

Many different approaches have been used to circumvent the present limitation of FPI's to low molecular weight substances. An early attempt to

develop FPI's for high molecular weight antigens was reported by Grossman. The dansyl (dimethylaminonaphthalene sulfonic acid) fluorophore was used because of its lifetime near 20 ns. Tsuruoka and coworkers attempted to develop a FPI with IgG by increasing the molecular weight of the antibody. This was accomplished by immobilizing the antibody with latex or colloidal silver. Urios and Cittanova decreased the size of the labeled antibody by using Fab fragments in place of complete IgG molecules. Another approach to enable the measurement of high-molecular-weight antigens was introduced by Wei and Herron. They used a tetramethylrhodamine-labeled synthetic peptide, which has a high binding affinity for the Ab of hCG (human chorionic gonadotrophin), as the tracer antigen in their FPI for hCG. In the assay, the tracer antigen, which has a low molecular weight, is replaced by hCG (high molecular weight) thus reducing the amount of polarization.

Since the basic theory of the depolarization of fluorescence through Brownian rotation was presented by Perrin in 1926, fluorescence anisotropy decay measurements have been widely used to study the rotational dynamics of proteins, membrane-bound proteins and other macromolecules. The use of the polarization of extrinsic fluorescent labels to study proteins was introduced by Weber and was applied to the characterization of a number of proteins by Weber and others.

There are limitations imposed by the short fluorescence lifetime that have been circumvented by use of phosphorescence anisotropy decays, which have been used to study the rotational dynamics of membrane-bound proteins. Such measurements are based

exclusively on the triplet probe eosin, which displays a millisecond phosphorescence decay time in the absence of oxygen. Rotational motions have been quantified by transient absorption anisotropy and by time-resolved phosphorescence anisotropy. There are, however, relatively few useful triplet probes. The use of phosphorescence is also inconvenient because of the need to rigorously exclude molecular oxygen, and the low initial phosphorescence anisotropies, typically 0.1 or smaller.

The polarized luminescence from metal ligand complexes has been used to study macromolecular dynamics. Studies have shown that ruthenium (Ru), rhenium (Re) and osmium (Os) metal ligand complexes display high anisotropy in the absence of rotational diffusion. Importantly, these metal ligand complexes display luminescence decay times ranging from 100 ns to 100  $\mu$ s. Consequently, these probes extend the observable timescale of anisotropy decay measurements by many-fold compared with that observable with routinely used fluorophores. As a result, metal ligand complexes have been used to measure rotational motion of proteins and probe the submicrosecond dynamics of DNA. Time-resolved anisotropy measurements have demonstrated that metal ligand complexes when covalently linked to human serum albumin (HSA), concanavalin A, human immunoglobulin G, and ferritin can be used to measure rotational motions on the 10 ns to 1.5  $\mu$ s timescale.

Conventional organic fluorophores typically have a lifetime in the range of 1-10 ns, generally absorb in the high energy range, and are not very photostable. These properties limit the ability of these fluorophores to study slower domain-to-domain motions

in proteins or the rotational motions of membrane-bound proteins. Furthermore the sensitivity of these fluorophores is also limited by interfering autofluorescence which also occurs at the 1-10 ns time scale.

There remains a need in the art for metal-ligand complex probes which display long absorption emission wavelengths, long lifetimes, high luminescence, and/or high quantum yields, for use as biomolecular probes, and/or for metal-ligand complex probes that can be used in fluorescence polarization immunoassays of high molecular weight analytes, and for metal-ligand complex probes that can be used as anisotropy probes for protein hydrodynamics.

#### SUMMARY OF THE INVENTION

In accordance with the present invention, a method of conducting an assay of a sample containing an analyte of interest includes the step of forming a mixture so as to bring a metal-ligand complex into interactive proximity (10 to 120 Å) with the sample containing the analyte of interest. The mixture is irradiated with electromagnetic light so as to induce emission of light indicative of the analyte of interest. The emitted light is measured, and the measurement of the emitted light is utilized to measure the analyte of interest. In accordance with one embodiment, the metal-ligand complex is selected from the group consisting of  $[\text{Re}(\text{bcp})(\text{CO})_3(4\text{-COOHpy})]^+$ ,  $[\text{Os}(\text{phen})_2(\text{aphen})]^{2+}$ ,  $[\text{Os}(\text{tpy})(\text{triphos})]^{2+}$ ,  $[\text{Os}(\text{tppz})_2]^{2+}$ , and  $[\text{Os}(\text{tppy})_2]^{2+}$ .

BRIEF DESCRIPTION OF THE DRAWINGS

FIG. 1 shows the molecular structure of  $[\text{Re}(\text{bcp})(\text{CO})_3(4\text{-COOHPy})]^+$ , which displays a high quantum yield near 0.5 in organic solutions and a lifetime near  $7\mu\text{s}$ .

FIG. 2 is a graph depicting the absorption and emission spectra of  $[\text{Re}(\text{bcp})(\text{CO})_3(4\text{-COOHPy})]^+$  in  $\text{CHCl}_3$ ,  $\text{CH}_3\text{CN}$ ,  $\text{CH}_3\text{OH}$ , and in buffer, at room temperature. The excitation wavelength was 400 nm. The solid line shows the excitation anisotropy spectrum in 100% glycerol at  $-60^\circ\text{C}$ , with the emission wavelength tuned to 550 nm. The bandpass was 8 nm for all measurements.

FIG. 3 graphically shows that in organic solutions,  $[\text{Re}(\text{bcp})(\text{CO})_3(4\text{-COOHPy})]^+$  is highly sensitive to dissolved oxygen, but in the absence of dissolved oxygen, it displays a lifetime over 7  $\mu\text{s}$ . The oxygen dependent spectra of the rhenium complex was taken at room temperature, excitation was 400 nm, and with a bandpass of 8 nm. The inset shows spectra obtained in air and oxygen.

FIG. 4 graphically shows the frequency-domain intensity decays of  $[\text{Re}(\text{bcp})(\text{CO})_3(4\text{-COOHPy})]^+$  in methanol. The lifetime is reduced to about 0.5 microseconds in the presence of dissolved oxygen from the atmosphere. The excitation was 390 nm and a 500 nm cutoff filter was used to isolate the emission.

FIG. 5 graphically shows the emission spectra of  $[\text{Re}(\text{bcp})(\text{CO})_3(4\text{-COOHPy})]^+$  when conjugated to phosphatidyl ethanolamine and embedded into DPPG vesicles. The mole ratio of the rhenium complex to phosphatidyl ethanolamine was 1:80. The excitation was 400 nm with a bandpass of 8 nm, measured at  $20^\circ\text{C}$ .

FIG. 6 graphically shows the lifetimes of  
[Re(bcp)(CO)<sub>3</sub>(4-COOHPy)]<sup>+</sup> labeled DPPG vesicles measured  
by the frequency-domain or phase-modulation method.  
Excitation was 340 nm and a 470 nm cutoff filter was  
5 used to isolate the emission.

FIG. 7 graphically shows that similar favorable  
properties were found for [Re(bcp)(CO)<sub>3</sub>(4-COOHPy)]<sup>+</sup> when  
conjugated to human serum albumin (HSA). The rhenium  
complex was conjugated to HSA in 0.1 M PBS buffer, pH  
10 7.0, and equilibrated with argon or air. The  
excitation wavelength was 400 nm with a bandpass of 8  
nm, at 20° C.

FIG. 8 graphically shows that the lifetime of  
[Re(bcp)(CO)<sub>3</sub>(4-COOHPy)]<sup>+</sup> when conjugated to HSA is near  
15 3 μs in the presence or absence of dissolved oxygen  
from the atmosphere. The excitation was 390 nm and a  
500 nm cutoff filter was used to isolate the emission.

FIG. 9 graphically depicts binding of  
[Re(bcp)(CO)<sub>3</sub>(4-COOHPy)]<sup>+</sup> labeled HSA to anti-HSA. The  
20 increase in polarization is due to binding of the  
antibody to HSA. This demonstrates the possibility of  
polarization immunoassays using this high quantum yield  
rhenium complex. The excitation wavelength was 400 nm  
and observation was 550 nm with a bandpass of 8 nm, at  
25 20°C.

FIG. 10 shows the chemical structure of  
[Os(phen)<sub>2</sub>(aphen)]<sup>2+</sup> and [Os(tpy)(triphos)]<sup>2+</sup>.

FIG. 11 graphically depicts the absorption spectra  
of red absorbing osmium probes in acetonitrile at room  
30 temperature.

FIG. 12 graphically shows the emission spectra of  
[Os(phen)<sub>2</sub>(aphen)]<sup>2+</sup>, [Os(tpy)(triphos)]<sup>2+</sup>, [Os(tppz)<sub>2</sub>]<sup>2+</sup>,  
and [Os(ttpy)<sub>2</sub>]<sup>2+</sup>.

FIG. 13 is a graph depicting the anisotropy spectra of  $[\text{Os}(\text{phen})_2(\text{aphen})]^{2+}$ ,  $[\text{Os}(\text{tpy})(\text{triphos})]^{2+}$ ,  $[\text{Os}(\text{tppz})_2]^{2+}$ , and  $[\text{Os}(\text{ttpy})_2]^{2+}$  in 9:1 glycerol:methanol at  $-55^\circ\text{C}$ .

5        FIG. 14 graphically depicts the intensity decay of long lifetime  $[\text{Os}(\text{tppz})_2]^{2+}$ .

FIG. 15 is an intuitive description of a fluorescence polarization immunoassay. Re-L is  $[\text{Re}(\text{bcp})(\text{CO})_3(4\text{-COOHPy})]^+$ , and  $\theta$  is the rotational correlation time.

FIG. 16 graphically shows molecular weight dependent anisotropy for a protein-bound luminophore with luminescence lifetimes of 4, 40, 400, and 2700 ns.

FIG. 17 shows the molecular structures of the ligands in  $[\text{Os}(\text{phen})_2(\text{aphen})]^{2+}$ ,  $[\text{Os}(\text{tpy})(\text{triphos})]^{2+}$ ,  $[\text{Os}(\text{tppz})_2]^{2+}$ , and  $[\text{Os}(\text{ttpy})_2]^{2+}$ .

FIG. 18 graphically depicts the absorption spectra of  $[\text{Re}(\text{bcp})(\text{CO})_3(4\text{-COOHPy})]^+$ , 2,9-dimethyl-4,7-diphenyl-1,10-phenanthroline (bcp), and isonicotinic acid (4-COOHPy) in methanol.

FIG. 19 graphically shows the temperature dependent emission spectra (top) and intensity-normalized emission spectra (bottom) of  $[\text{Re}(\text{bcp})(\text{CO})_3(4\text{-COOHPy})]^+$  in 100% glycerol. Excitation was 360 nm with a bandpass of 8 nm.

FIG. 20 depicts the temperature-dependent emission anisotropy of  $[\text{Re}(\text{bcp})(\text{CO})_3(4\text{-COOHPy})]^+$  in solutions composed of different ratios of glycerol/ $\text{H}_2\text{O}$  (v/v). Emission was monitored at 550 nm with an excitation wavelength of 400 nm and a bandpass of 8 nm.

FIG. 21 graphically shows excitation spectra and  $R(\lambda)$  values for  $[\text{Re}(\text{bcp})(\text{CO})_3(4\text{-COOHPy})]^+$  in  $\text{CH}_3\text{CN}$ .

FIG. 22 depicts the emission anisotropy spectrum of  $[\text{Re}(\text{bcp})(\text{CO})_3(4\text{-COOHPy})]^+$  in 100% glycerol at  $-60^\circ\text{C}$ .

An emission spectrum is shown for comparison.  
Excitation was 400 nm with a bandpass of 8 nm.

FIG. 23 graphically shows the absorption and  
emission spectra of  $[\text{Re}(\text{bcp})(\text{CO})_3(4\text{-COOHPy})]^+$  conjugated  
5 to HSA in 0.1 M PBS buffer, pH 7.0. Excitation  
wavelength was 400 nm. The solid line shows the  
excitation anisotropy spectrum in 100% glycerol at -  
60°C, with an emission wavelength of 550 nm. The  
bandpass was 8 nm for all measurements.

10 FIG. 24 graphically depicts the steady-state  
fluorescence polarization of Re-HSA added to  
preincubated mixtures of anti-HSA with various  
concentrations of unlabeled HSA. The excitation  
wavelength was 400 nm and the observation wavelength  
15 was 550 nm with a bandpass of 8 nm, at 20°C. Error  
bars represent the standard deviations of three  
polarization readings.

FIG. 25 shows the absorption spectra of  
 $[\text{Re}(\text{bcp})(\text{CO})_3(4\text{-COOHPy})]^+$ , 2,9-dimethyl-4,7-diphenyl-  
20 1,10-phenanthroline (bcp), and isonicotinic acid (4-  
COOHPy) in methanol. The solid line shows the  
excitation spectrum of  $[\text{Re}(\text{bcp})(\text{CO})_3(4\text{-COOHPy})]^+$  in  
methanol.

FIG. 26 depicts the intensity-normalized emission  
25 spectra of free  $[\text{Re}(\text{bcp})(\text{CO})_3(4\text{-COOHPy})]^+$  in  $\text{CHCl}_3$ ,  
 $\text{CH}_3\text{OH}$ , and Re-labeled proteins, Re-HSA and Re-IgG in 0.1  
M PBS buffer.

FIG. 27 graphically shows the excitation  
anisotropy spectra of free  $[\text{Re}(\text{bcp})(\text{CO})_3(4\text{-COOHPy})]^+$  in  
30 100% glycerol and Re-labeled proteins in 60%  
glycerol/40% 0.1 M PBS buffer (v/v) with an excitation  
band pass of 8 nm, at -60°C.

FIG. 28 depicts the temperature-dependent emission  
anisotropy of free  $[\text{Re}(\text{bcp})(\text{CO})_3(4\text{-COOHPy})]^+$  and its

protein conjugates in 60% glycerol/40% 0.1 M PBS buffer (v/v). Excitation wavelength was  $400 \pm 4$  nm; emission wavelength was  $550 \pm 4$  nm.

FIG. 29 shows the anisotropy decays of free  
5 [Re(bcp)(CO)<sub>3</sub>(4-COOHPy)]<sup>+</sup> at the indicated solutions and the indicated temperatures.

FIG. 30 graphically shows the anisotropy decays of Re-labeled proteins in buffer (top) and in the indicated solutions (bottom).

#### 10 DETAILED DESCRIPTION OF THE INVENTION

Metal-ligand complexes offer advantages for optical sensing because they allow lifetime based sensing with low cost instrumentation. Many of these complexes display polarized emission. Polarized  
15 emission is valuable because it enables these compounds to be used for polarization immunoassays.

The metal-ligand complex probes of the invention have applications in biophysics, clinical chemistry, and immunoassays. The complexes of the platinum  
20 metals, Ru(II), Os(II), and Re(I), display anisotropy properties that can be successfully utilized in fluorescence polarization immunoassays and in studies of protein and/or lipid hydrodynamics. The complexes can be comprised of mono, bis, or tris(heteroleptic)  
25 complexes of Ru(II) and Os(II) and carbon monoxide diimine complexes of Re(I). The metal-ligand complexes include the high quantum yield rhenium (I) complex of the formula [Re(bcp)(CO)<sub>3</sub>(4-COOHPy)]<sup>+</sup> and the long lifetime osmium (II) complexes, [Os(phen)<sub>2</sub>(aphen)]<sup>2+</sup>,  
30 [Os(tpy)(triphos)]<sup>2+</sup>, [Os(tppz)<sub>2</sub>]<sup>2+</sup>, and [Os(ttpy)<sub>2</sub>]<sup>2+</sup>.

The ligands covalently bound to the metals can include ligands based on diimine, phosphine, arsine, pyridine, substituted pyridines, carbon monoxide,

carbonyl, and any combination thereof. The ligands may be substituted with functional groups that can be directly conjugated to macromolecules such as amine reactive N-hydroxysuccidimide, isothiocyanate, sulfonyl chloride containing ligands, sulfhydryl reactive iodoacetamide, and maleimide containing ligands.

These long lifetime metal-ligand complexes offer advantages for optical sensing because they allow lifetime based sensing with low cost instrumentation. These new probes can be used in biophysical chemistry, immunoassays of high molecular weight antigens, with red laser diode, red LED, or blue or ultraviolet LED excitation, and in lifetime immunoassays with improved spectral properties.

$[\text{Re}(\text{bcp})(\text{CO})_3(4\text{-COOHPy})]^+$  displays a quantum yield and lifetime considerably longer than that available with previous metal-ligand complexes. The lifetimes of  $[\text{Os}(\text{phen})_2(\text{aphen})]^{2+}$ ,  $[\text{Os}(\text{tpy})(\text{triphos})]^{2+}$ ,  $[\text{Os}(\text{tppz})_2]^{2+}$ , and  $[\text{Os}(\text{ttpy})_2]^{2+}$  are longer than that available with previous osmium complexes.

A favorable property of  $[\text{Re}(\text{bcp})(\text{CO})_3(4\text{-COOHPy})]^+$  is that it is not as severely quenched by oxygen in aqueous solution when bound to biological molecules. The lifetimes of rhenium labeled DPPG vesicles can exceed 3  $\mu\text{s}$  in oxygenated aqueous solution, and their quantum yield is 0.2 or larger in oxygenated solutions. This rhenium (I) complex displays a four fold higher quantum yield and an eight fold longer lifetime compared to prior art rhenium (I) complexes. Rhenium labeled HSA is only moderately quenched by dissolved oxygen, and the average lifetime is near 3  $\mu\text{s}$ .

$[\text{Os}(\text{phen})_2(\text{aphen})]^{2+}$  and  $[\text{Os}(\text{tpy})(\text{triphos})]^{2+}$  display a quantum yield of 0.02, which is larger than

the quantum yield of previous osmium complexes, in which the quantum yield was less than 0.001.

The absorption spectra of  $[\text{Os}(\text{phen})_2(\text{aphen})]^{2+}$ ,  $[\text{Os}(\text{tpy})(\text{triphos})]^{2+}$ ,  $[\text{Os}(\text{tppz})_2]^{2+}$ , and  $[\text{Os}(\text{ttpy})_2]^{2+}$  extend to 700 nm which allows them to be used with long wavelength excitation. The emission of these osmium (II) complexes above 650 nm is desirable for avoiding autofluorescence from biological samples and for use with non-invasive transdermal sensing. The high anisotropy of these osmium complexes near 0.3 makes them useful in fluorescence polarization immunoassays. It is desirable to have probes which display long absorption emission wavelengths and also display long lifetimes. The lifetime of  $[\text{Os}(\text{tppz})_2]^{2+}$  is near 150 ns, which is 10-fold larger than obtained with prior art osmium (II) complexes, which displayed a lifetime of 14 ns. The long lifetime permits such probes to be used with gated detection to avoid interfering autofluorescence.

Luminescence probes have high sensitivity and specificity. Luminescence probes based on metal-ligand complexes are valuable in biochemistry and biophysics.

The invention is applicable to long-lived, highly luminescent rhenium (I) metal-ligand complexes as biomolecular probes.

The newly synthesized rhenium(I) metal-ligand complex  $[\text{Re}(\text{bcp})(\text{CO})_3(4\text{-COOHPy})]$ , where bcp is 2,9-dimethyl-4,7-diphenyl-1,10-phenanthroline and 4-COOHPy is isonicotinic acid, exhibits high quantum yields, long lifetimes, and high anisotropy in the absence of rotational diffusion, and can be conjugated to proteins and lipids.

The flexibility in selection of the metal and the ligand renders metal-ligand complexes a versatile class of biomolecular probes. A wide range of lifetimes, absorption and emission spectra, and polarization characteristics offers numerous experimental opportunities in biophysics and clinical chemistry. For instance, a long lifetime is desirable for fluorescence polarization immunoassays of high-molecular-weight antigens, whereas a long wavelength is favorable for non-invasive clinical applications, due to lower autofluorescence and higher tissue transmission at longer wavelengths.

With its high quantum yields, long lifetimes, as well as its highly polarized emission, this rhenium (I) complex may expand the measurement of rotational motions to timescales  $> 10 \mu\text{s}$  when bound to macromolecules.

The use of such metal-ligand complexes enable fluorescence polarization immunoassays to bypass the usual limitation to low-molecular-weight antigens. The usual limitation is a consequence of the  $< 10 \text{ ns}$  decay times of the previously used fluorophores.

The invention is also applicable to fluorescence polarization immunoassays of high molecular weight analytes.

A new FPI probe,  $[\text{Re}(\text{bcp})(\text{CO})_3(4\text{-COOHpy})](\text{ClO}_4)$ , for high molecular weight antigens has been synthesized. This Re(I) complex displays highly polarized emission (with a maximum polarization near 0.4 and maximum anisotropy near 0.3) in the absence of rotational diffusion and a long average lifetime (2.7  $\mu\text{s}$ ) when bound to proteins in air-equilibrated aqueous solution. The steady-state polarization of the Re(I)

complex labeled HSA conjugate (Re-HSA) was sensitive to the binding of anti-HSA, resulting in a significant increase in luminescence polarization. The labeled HSA was also used in a competitive format with unlabeled

5 HSA acting as an antigen. More importantly, the lifetime of this probe when covalently labeled to HSA in air-equilibrated aqueous solution is near 3  $\mu$ s, which theoretically allows immunoassays of antigens with molecular weights up to  $10^6$  Daltons (Figure 16).

10 The fluorescence polarization ( $P$ ) of a labeled macromolecule depends on the fluorescence lifetime ( $\tau$ ) and the rotational correlation time ( $\theta$ ):

$$\left( \frac{1}{P} - \frac{1}{3} \right) = \left( \frac{1}{P_0} - \frac{1}{3} \right) \left( 1 + \frac{\tau}{\theta} \right) \quad (1)$$

where  $P_0$  is the polarization observed in the absence of rotational diffusion. The effect of molecular weight on the polarization values can be seen from an  
 5 alternative form of Equation 1:

$$\left( \frac{1}{P} - \frac{1}{3} \right) = \left( \frac{1}{P_0} - \frac{1}{3} \right) \left( 1 + \frac{kT}{\eta V \tau} \right) \quad (2)$$

where  $k$  is the Boltzmann constant,  $T$  is the absolute temperature in Kelvin,  $\eta$  is the viscosity of the solution, and  $V$  is the molecular volume. The molecular  
 10 volume of the protein is related to the molecular weight ( $M_r$ ) and the rotational correlation time by:

$$\theta = \frac{\eta V}{kT} = \frac{\eta M_r}{RT} (\bar{v} + h) \quad (3)$$

where  $R$  is the ideal gas constant,  $\bar{v}$   
 15 is the specific volume of the protein, and  $h$  is the hydration, typically 0.2 g H<sub>2</sub>O/1 g protein. Generally, the observed correlation times are about twofold longer than those calculated for an anhydrous sphere (Eq. 3 with  $h=0$ ) due to the effects of hydration and the  
 20 nonspherical shapes of most proteins. Therefore, in aqueous solution at 20°C ( $\eta=1\text{cP}$ ), one can expect a protein such as HSA ( $M_r \sim 65,000$  Da, with  
 $\bar{v} + h = 1.9$ ) to display a rotational correlation time near 50 ns.

The advantage of using a luminophore with a long lifetime is illustrated by comparing the expected polarization values for materials with different molecular weights, labeled with probes with different lifetimes, Figure 16. It is convenient to use the anisotropy ( $r$ ) in this calculation. The anisotropy and polarization are related by:

$$P = \frac{I_{\parallel} - I_{\perp}}{I_{\parallel} + I_{\perp}} \quad (4)$$

$$r = \frac{I_{\parallel} - I_{\perp}}{I_{\parallel} + 2I_{\perp}} \quad (5)$$

where  $I_{\parallel}$  and  $I_{\perp}$  are the vertically and horizontally polarized components of the emission. The values of  $P$  and  $r$  can be interchanged using:

$$r = \frac{2P}{3-P} \quad (6)$$

$$P = \frac{3r}{2+r} \quad (7)$$

The parameters  $P$  and  $r$  are both commonly used to describe rotational diffusion processes of fluorophores in solution. The values of  $P$  are more often used in FPI because they are entrenched by tradition and are slightly larger than the anisotropy values. The parameter  $r$  is preferred on the basis of theory. The anisotropy of a labeled macromolecule is:

$$r = \frac{r_0}{1 + \tau/\theta} \quad (8)$$

where  $r_0$  is the anisotropy in the absence of rotational diffusion and is typically near 0.3 for most fluorophores, although the theoretical limit given  
5 colinear transition dipoles for absorption and emission is 0.4.

The expected anisotropy values for a range of photoluminescence lifetimes were simulated. These calculations were based on Equations 3 and 8,  
10  $\bar{v}$  established on the assumptions that the limiting anisotropy ( $r_0$ ) was 0.3 in the absence of rotational diffusion, the solution viscosity was 1 cP, and  $+h = 1.9$  for the protein. These simulations demonstrate how the lifetime of the luminophore  
15 determines the range of molecular weights which can be resolved by the luminophore in an immunoassay. Presently, most immunoassays rely on fluorescein and rhodamine derivatives as fluorescent probes ( $\tau \sim 4$  ns). If one considers that most low molecular weight  
20 antigens are in the range of  $< 1000$  Da, the expected anisotropy of the labeled antigen can be estimated from Figure 16 to be in the range of 0.05. Upon antigen association with antibody, the molecular weight increases ( $M_r \sim 160,000$  Da) and the anisotropy of the  
25 bioconjugate approaches 0.30. Hence, a large change in anisotropy is found upon binding of Ag to Ab for low molecular weight antigens, when utilizing a 4 ns lifetime fluorophore.

However, if the molecular weight of the labeled  
30 antigen is larger, above 20,000 Da, then the anisotropy changes only slightly upon binding to antibody, if the

same fluorophore is used. For instance, suppose the molecular weight of the labeled antigen is 160,000 Da, with a rotational correlation time of 125 ns, and that of the antibody-bound form is 600,000 Da, with a rotational correlation time of 470 ns. In this particular case, the anisotropy values will differ by less than 2% between the two forms using a short lifetime fluorophore. This small change is attributed to the large discrepancy between the lifetime of the fluorophore and the rotational correlation time of the labeled macromolecular complex. It is this reason why FPI's are performed only in the low molecular weight range with conventional short lifetime fluorophores.

The lifetime of the luminophore  $[\text{Re}(\text{bcp})(\text{CO})_3(4\text{-COOHpy})]^{+}$  is in the range of 3  $\mu\text{s}$ . For the example described above, the binding assay would now be detectable using luminescence polarization (Figure 16). Theoretically, a luminophore with a lifetime of 3  $\mu\text{s}$  could allow the analysis of biological systems with molecular weights up to 100 million Daltons and correlation times up to 80  $\mu\text{s}$ , thereby greatly expanding the capabilities of FPI's to include the study of entire cells, viruses, and other large biomolecules and biomolecular complexes.

The superior approach for the direct measurement of high molecular weight analytes in an immunoassay is to develop luminescence probes with lifetimes that are comparable to the rotational correlation times of the antibody, antigen, and the bioconjugates they form. The use of the photoluminescence from metal-to-ligand charge transfer (MLCT) excited states in this regard is definitely the proper direction of this research. The sensitivity and dynamic range of a generic immunoassay can be correlated well to the lifetime of the probe

used and the hydrodynamic volumes (molecular weight) of the bound and free tracer antigen (Figure 16). To observe comparable anisotropy values for a 2.7  $\mu$ s probe as that of a 4 ns probe, the molecular weight range can be at least 3 orders of magnitude larger in the former case.

Two disadvantages of MLCT complexes are their low extinction coefficients and quantum yields when compared to a probe like fluorescein. The extinction coefficients of MLCT compounds are generally 2-5 fold lower than fluorescein. There is generally about a 10-fold difference in quantum yield between fluorescein and MLCT compounds. However, these disadvantages are offset by the fact that the photostability of MLCT complexes is remarkable compared to fluorescein, and MLCT compounds do not display any probe-probe interactions, quite unlike fluorescein, which allows for a much larger dye:protein ratio when labeling with MLCT complexes. In addition, the long-lifetimes of MLCT complexes allow for the off-gating of the autofluorescence from biological samples which takes place in the 1-10 ns timescale, which is not possible with fluorescein.

MLCT probes display lifetimes that range from sub-nanosecond to >100  $\mu$ s. Therefore, MLCT compounds can be specifically tailored to be used in any immunoassay. MLCT compounds can be systematically engineered to alter their spectroscopic, photophysical, and chemical properties. The spectral and chemical versatility of MLCT complexes allows the design of probes displaying lifetimes that respond to specific molecular weights. Compared to  $[\text{Ru}(\text{bpy})_2(\text{dcb})]^{2+}$ ,  $[\text{Re}(\text{bcp})(\text{CO})_3(4\text{-COOHPy})]^+$  displays higher quantum yield, higher anisotropy, and longer lifetime. The quantum yields of

$[\text{Ru}(\text{bpy})_2(\text{dcb})]^{2+}$  and  $[\text{Re}(\text{bcp})(\text{CO})_3(4\text{-COOHPy})]^+$  are about 0.05 and 0.12, respectively, when bound to protein.

The invention is applicable to anisotropy probes for protein hydrodynamics.

5       The newly made Re-complex,  $[\text{Re}(\text{bcp})(\text{CO})_3(4\text{-COOHPy})](\text{ClO}_4)$ , can be used as an anisotropy probe for protein hydrodynamics.  $[\text{Re}(\text{bcp})(\text{CO})_3(4\text{-COOHPy})]^+$  displays highly polarized emission with a maximal anisotropy near 0.3 in frozen solution, thus making it  
10       useful as an anisotropy probe.  $[\text{Re}(\text{bcp})(\text{CO})_3(4\text{-COOHPy})]^+$  was conjugated to human serum albumin (HSA) and bovine immunoglobulin G (IgG). Long excited-state lifetimes in fluid solutions equilibrated with air at room temperature were found for  $[\text{Re}(\text{bcp})(\text{CO})_3(4\text{-COOHPy})]^+$  when covalently linked to HSA and IgG.  
15       Analyses of the anisotropy decays of the protein conjugates demonstrate that  $[\text{Re}(\text{bcp})(\text{CO})_3(4\text{-COOHPy})]^+$  can be used to measure rotational motions on the 10 ns to ~100  $\mu\text{s}$  timescale in air equilibrated solutions.

20        $[\text{Re}(\text{bcp})(\text{CO})_3(4\text{-COOHPy})]^+$  can be used as an anisotropy probe for macromolecular dynamics. The anisotropy decays are dependent on protein dynamics. The correlation time has been extended to 100  $\mu\text{s}$ , which has been inaccessible with routinely used nanosecond  
25       probes. This metal-ligand complex, with its high quantum yield, long lifetime, and highly polarized emission has opened a new timescale regime for the study of macromolecular dynamics.

30       The usefulness of the fluorescence anisotropy measurements is derived from its dependence on the extent of rotational diffusion during the lifetime of the excited state. Two basic kinds of information may be derived from fluorescence anisotropy decay

measurements. Anisotropy decay may provide information as to the size and shape factor of macromolecules, reflecting the macromolecule and the attached fluorophore which rotate as a unit. Anisotropy decays  
5 may also provide information about the internal rotational motions present in the macromolecules and the nature of the molecular flexibility. Information about the rotational motion is available over a time range extending to about 3 times the fluorescence  
10 lifetime, after which there is too little signal for accurate anisotropy measurements. Because the lifetime of typical fluorophores ranges from 1 to 10 ns, it is difficult to measure rotation correlation times larger than 30 ns. Therefore, it is difficult to determine  
15 the rotational hydrodynamics of larger proteins or membrane-bound proteins.

The invention also is applicable to red fluorescent dyes for biophysics and for sensors.

Several polypyridine compounds of osmium(II) have  
20 been synthesized. These compounds can be conjugatable to proteins, typically absorb above 550 nm, emit above 700 nm and their lifetimes are higher than 50 ns. The emission of these compounds is polarized, so they have excellent applications as LED excitable and red  
25 emitting dyes for biophysical experiments. The low energy absorption as well as emission and high lifetime can be used for lifetime based oxygen sensing.

We have developed rhenium and osmium metal ligand complexes which are very photostable, have polarized  
30 emission and long decay times. The longer decay times allow increased sensitivity using gated detection following decay of the unwanted autofluorescence. Some lanthanide chelates compounds show longer decay times

which allow gated detection and increased sensitivity for immunoassays, but do not display polarized emission, which is required for protein hydrodynamics.

5 The dyes consist of MLCT complexes of osmium(II) metal with polypyridine and nonchromophoric tridentate phosphine ligands. Figure 17 represents the structure of all ligands used, and Figure 10 represents the structure of two complexes of each class. All these complexes show good fundamental anisotropy ( $r_0$ ) and long  
10 decay times. Therefore, they can be used in biophysics to study the hydrodynamics of macromolecules. Another added advantage of using these complexes is their high photo-stability in solvents.

The long lifetimes of rhenium (I), ruthenium (II)  
15 and osmium (II) complexes allow their use as oxygen sensors. The effect of oxygen on osmium complexes is less than its effect on the analogous ruthenium complexes because of shorter excited state lifetimes. The lifetime of these complexes is long enough to use  
20 them as oxygen sensors for lifetime based sensing using low-cost phase fluorometry with red emitting, LED light sources. The effect of oxygen on  $[\text{Os}(\text{tppz})_2]^{2+}$  is represented in Figure 14.

Because of their long decay lifetimes, diode laser  
25 excitability (absorb at 500 -700 nm), low energy emission (emit in red region, 700-750 nm), reasonable quantum yields, polarized emission (anisotropy 0.15-0.35) and high photo-stability, these osmium(II) polypyridine complexes can be used as fluorophores in  
30 biophysical applications. These complexes can be used as red fluorophores for macromolecules. When using these fluorophores, one can avoid low signal to noise level by using gated observation. Another advantage of

these compounds is high photostability. These dyes can be handled in room light for months.

These metal ligand complexes can be prepared with different functional groups for conjugation to biological macromolecules. These include isothiocyanate, sulfonyl chlorides, iodoacetamides, and malimides. Also, the organic ligands bound to the rhenium and osmium atoms can be varied to further modify the absorption and emission spectral properties. The invention is further illustrated by the following examples, which are not intended to be limiting.

Example 1:

*A Long-Lived, Highly Luminescent Rhenium (I) Metal-Ligand Complex As A Biomolecular Probe*

Human serum albumin (HSA), bovine immunoglobulin G (IgG), dipalmitoyl-L- $\alpha$ -phosphatidylethanolamine (PE) and dipalmitoyl-L- $\alpha$ -phosphatidylglycerol (DPPG) were obtained from Sigma Chemical Co. and were used without further purification. 2,9-dimethyl-4,7-diphenyl-1,10-phenanthroline (bcp), isonicotinic acid (4-COOHPy),  $\text{AgClO}_4$ ,  $\text{NH}_4\text{PF}_6$ , and  $\text{Re}(\text{CO})_5\text{Cl}$  were obtained from Aldrich and used as received. The other solvents used were of HPLC or spectroscopic reagent grade. FTIR spectra were obtained on a Perkin Elmer 1600 Series spectrophotometer with 4  $\text{cm}^{-1}$  resolution. Samples were dissolved in dichloromethane and measured in a liquid cell.

*Re(bcp) (CO<sub>2</sub>)<sub>3</sub>Cl Synthesis*

Re(CO)<sub>5</sub>Cl (1 g, 2.76 mmol) was reacted with bcp(1.05 g, 2.9 mmol) in toluene under reflux with stirring for 1 hour. The solution was cooled to room temperature and hexane was added which precipitated a yellow solid. This was collected on a coarse frit and washed with toluene followed by hexane. The product was dried under vacuum. Yield: 1.52 g (83%). Anal. Calcd for ReC<sub>29</sub>H<sub>20</sub>N<sub>2</sub>O<sub>2</sub>Cl: C, 52.29; H, 3.03; N, 4.21. Found: C, 52.04; H, 2.93; N, 3.95. IR (νCO: 2021(vs), 1914(vs), 1895(vs) cm<sup>-1</sup>).

*Re(bcp) (CO<sub>3</sub>) (PyCOOH) Synthesis*

Re(bcp) (CO)<sub>3</sub>Cl (1.5 g, 2.25 mmol), AgClO<sub>4</sub> (514 mgs, 2.48 mmol), and 4-COOHPy (8.3 g, 67.5 mmol) were refluxed in 4:1 MeOH:toluene under argon in the dark for 24 hours. This was cooled to room temperature and filtered to remove the AgCl precipitate. The filtrate was rotovaped to dryness and the solid resuspended in CH<sub>2</sub>Cl<sub>2</sub> and filtered (to remove 4-COOHPy). The filtrate was rotovaped to dryness and a bright yellow solid was obtained. Yield: 1.8 g (94 %). Anal. Calcd for ReC<sub>35</sub>H<sub>25</sub>N<sub>3</sub>O<sub>9</sub>Cl: C, 49.27; H, 2.95; N, 4.92. Found: C, 50.30; H, 2.98; N, 4.80. IR (νCO: 2034(vs), 2022(vs), 1919(vs) cm<sup>-1</sup>). FAB-MS[M-ClO<sub>4</sub><sup>-</sup>]:755. The hexafluorophosphate salt was prepared by methathesis of the perchlorate salt by dissolving it in 1:1 acetone:H<sub>2</sub>O and precipitating it by the addition of a concentrated aqueous solution of NH<sub>4</sub>PF<sub>6</sub>. High purity luminescence samples were prepared using chromatography procedures previously described in the literature. (Wallace, L., and Rillema, D.P. (1993) *Inorg. Chem.* 32, 3836-3843; Sacksteder, L., Zipp, A.P., Brown, E.A., Streich, J.

Demas, J.N., and DeGraff, B.A. (1990) *Inorg. Chem.* 29, 4335-4340).

*Preparation of Activated Succimidyl Ester*

5 mg of N,N'-dicyclohexylcarbodiimide (DCC) and 3  
5 mg of N-hydroxy-succinimide (NHS) were dissolved in  
0.15 ml of DMF with stirring, 10 mg of the Re-complex  
in 0.15 ml of DMF was then added, and the mixture was  
stirred for a few hours. The formed precipitate was  
removed by filtration through a syringe filter, and the  
10 filtrate containing the active Re-complex was used for  
labeling the substrates.

The proteins HSA and IgG (10 mg of protein) were  
labeled by adding a 15-fold molar excess of the Re-NHS  
in 50  $\mu$ l of DMF to 1 ml of stirred protein solution  
15 (0.2 M carbonate buffer, pH 8.5), followed by a 5 h  
incubation and purification of the labeled protein by  
gel filtration chromatography on Sephadex G-25, using  
0.1 M PBS, pH 7.0. Our 0.1 M PBS (phosphate buffered  
saline) consisted of 0.1 M  $\text{NaH}_2\text{PO}_4$  and 0.1 M  $\text{NaHPO}_4$  in  
20 deionized water. The dye:protein ratio of the Re-HSA  
conjugate was determined to be 2:1. The concentration  
of the protein was determined by the Coomassie Plus  
Protein Assay (Pierce) and the concentration of the  
Re(I) complex was determined by its absorbance at 400  
25 nm ( $\epsilon = 5040 \text{ M}^{-1}\text{cm}^{-1}$ ), assuming the same extinction  
coefficient as the free complex.

95 mg of the Re-complex and 13 mg of NHS were  
dissolved in 0.7 ml of  $\text{CHCl}_3$  at room temperature, 24 mg  
of DCC was then added. The mixture was sealed and  
30 stirred for a few hours. The formed precipitate was  
removed by filtration through a syringe filter, and the  
filtrate containing the active Re-complex was slowly  
added to a stirred solution of PE (60 mg in 7.5 ml of

CHCl<sub>3</sub>) and triethylamine (4.5 ml) under an argon atmosphere. The mixture was stirred for 20 h in the dark. The solvents were removed under vacuum and the product was redissolved in 1.0 ml of CHCl<sub>3</sub>/MeOH

5 (1/1,v/v). The pure Re-PE was obtained by TLC on K6F silica gel plates using CHCl<sub>3</sub>/CH<sub>3</sub>OH/NH<sub>3</sub>OH (65/25/4, v/v/v) as the developing solvent. The R<sub>f</sub> value of the product is about 0.91, relative to that of PE (0.55).

For vesicle preparation, lipids with a Re-  
10 lipid/DPPG mole ratio of 1:200 were dissolved in CHCl<sub>3</sub>, and the solvent was removed by a stream of argon. Vesicles were prepared by sonicating in 10 mM Tris, 50 mM KCl, pH 7.5, at a final lipid concentration of 2 mg/ml of DPPG. The DPPG vesicles in the absence of Re-  
15 lipid did not display significant emission signals (< 2 %) under the present experimental conditions. Before sonication, the lipid and Re-complex were vacuum dessicated overnight to remove any traces of organic solvent. The vesicle solutions were deoxygenated by  
20 bubbling argon for 20 minutes, followed by equilibration with an argon atmosphere for 20 minutes, and then a subsequent 20 minute bubbling of the solution with argon.

Emission spectra were recorded on a SLM AB-2  
25 spectrofluorimeter. The frequency-domain instrumentation (ISS) was used for measurements of luminescence intensity decays. The frequency-domain lifetime measurements of the free dye in solution were performed on an ISS (Champaign, IL) K2 fluorimeter,  
30 using a Panasonic high intensity blue LED (light-emitting diode) configured to provide amplitude modulated light centered at 390 nm. (Sipior, J., Carter, G.M., Lakowicz, J.R., and Rao, G. (1997) Rev. Sci. Instrum. 68(7), 2666-2670). An Andover (Salem,

NH) 500 nm long-wave pass filter (500FH90-50S) was used to isolate the emission. For DPPG vesicle samples, frequency-domain lifetime measurements were performed using a Xenon arc lamp (300W) as the light source. The  
 5 excitation was amplitude modulated by an electro-optical low-frequency modulator (K2.LF from ISS) using  $340 \pm 8$  nm as the excitation wavelength. A 470 nm long-pass filter (Corning 3-71) was used to isolate the emission.

10 The frequency-domain intensity data were fitted by a nonlinear least squares procedure and were modeled with single and multi-exponential decay laws. The intensity decays were described by

$$I(t) = \sum_i \alpha_i e^{-t/\tau_i}$$

15

(9)

where  $I(t)$  is the luminescence intensity at time  $t$ ,  $\alpha_i$  and  $\tau_i$  are the pre-exponential weighting factors and the excited-state lifetimes, respectively. The subscripts denote individual components. Mean lifetimes were  
 20 calculated using Equation 9.

$$\langle \tau \rangle = \frac{\sum_i \alpha_i \tau_i^2}{\sum_i \alpha_i \tau_i} \quad (10)$$

The measured excitation anisotropy spectra are defined by Equation 5, where  $I_{\parallel}$  and  $I_{\perp}$  are the emission intensities measured with vertically polarized  
 25 excitation and the emission polarization parallel ( $I_{\parallel}$ ) or perpendicular ( $I_{\perp}$ ) to the excitation. The values of the polarized intensities were corrected for the

transmission efficiency of the polarized components by the detection optics.

As a probe of emission heterogeneity, the excitation spectra method described by Demas and co-workers (Sacksteder, L., Demas, J.N., and DeGraff, B.A. (1989) *Inorg. Chem.* 28, 1787-1792) was used. In brief, two uncorrected excitation spectra were measured with different emission wavelengths ( $\lambda_1$  and  $\lambda_2$ ).  $R(\lambda)$  is calculated as

$$R(\lambda) = E_1(\lambda) / E_2(\lambda) \quad (11)$$

where the  $E$ 's are the emission intensities while exciting at  $\lambda$  and monitoring at two different wavelengths,  $\lambda_1$  and  $\lambda_2$ . Since the sample absorbance and excitation intensities are the same at each excitation wavelength,  $R$  is related to the relative contributions of different emission components. If there is no ground-state heterogeneity or the equilibration in the excited state is rapid relative to sample decay times,  $R(\lambda)$  is wavelength independent. If there are multiple ground-state species that fail to equilibrate in their excited states,  $R(\lambda)$  varies with  $\lambda$ .

The molecular structure of  $[\text{Re}(\text{bcp})(\text{CO})_3(4\text{-COOHPy})]^+$  is shown in Figure 1. The absorption spectrum of the Re-complex in  $\text{CH}_3\text{OH}$  is shown in Figure 18. The absorption spectra of the ligands in  $\text{CH}_3\text{OH}$  are also shown for comparison. The spectra are normalized to unity to facilitate comparison. The maximum of the low-energy absorption band around 340 ~ 450 nm and the more intense higher energy absorption at 298 nm are the characteristic MLCT and  $\pi\text{-}\pi^*$  bands, respectively. It

is important to note that this complex can be excited with the UV output of a blue light emitting diode.

The excitation and emission spectra of the Re complex in  $\text{CHCl}_3$ ,  $\text{CH}_3\text{OH}$  and  $\text{CH}_3\text{CN}$  are shown in Figure 2. The large Stokes' shift of this Re complex (~100 nm) makes it a good candidate for energy transfer studies as there is no possibility for self-quenching. Also, the large Stokes' shift indicates a macromolecule can be labeled with multiple MLCT without self-quenching. This emission of this complex displays a strong sensitivity to local environment, as observed from the spectral shift of 539 nm in  $\text{CHCl}_3$  to 559 nm in 0.1 M PBS buffer solution at room temperature. When bound to biomolecules it is reasonable to expect that this complex's emission may respond to the subtle changes in the micro-environment of a biological sample. The emission intensity is strongly dependent on temperature as shown by the increased intensity at -57 °C compared with 19 °C (Figure 19). There is also a significant blue-shift in emission maximum with decreasing temperature (Figure 19). These results are consistent with the temperature dependence of many other MLCT complexes, wherein the energy gap between the ground and excited states increases with decreasing temperature resulting in a blue-shifted emission spectrum, increased lifetime, and higher quantum yield.

The lifetimes and quantum yields for  $[\text{Re}(\text{bcp})(\text{CO})_3(4\text{-COOHPy})]^+$  are summarized in Table 1.

Table 1. Photoluminescence quantum yields and lifetimes of  $\text{Re}(\text{bcp})(\text{CO})_3(4\text{-COOHpy})(\text{PF}_6)$  at room temperature unless otherwise indicated.

	Solvent	Conditions	$\phi^a$	$\tau(\mu\text{s})$	mean $\tau(\mu\text{s})$
5	$\text{CH}_3\text{OH}$	Air	0.039	0.54	
		Argon	0.54	7.25	
	$\text{CHCl}_3$	Air	0.047	0.66	
		Argon	0.55	6.72	
	$\text{CH}_3\text{CN}$	Air	0.016	0.49	
		Argon	0.23	4.65	
	Glycerol	Air	0.27	10.8	
10	Re-PE in DPPG vesicles	Air	0.13 (22°C)		4.36 (2°C)
					3.31 (10°C)
					2.54 (22°C)
					1.99 (35°C)
					1.82 (50°C)
		Argon	0.27		
	Re-IgG	Air	0.12		2.92
		Argon	0.22		4.07
	Re-HSA	Air	0.20		2.75
		Argon			3.44
	0.1 M PBS	Air		0.99	

15 <sup>a</sup> Absolute quantum yields are difficult to determine in the presence of uncertain amounts of dissolved oxygen under air-equilibrated conditions.

20 Demas and co-workers have demonstrated that certain rhenium complexes display high quantum yields, in excess of 0.7, and long lifetimes in excess of 10  $\mu\text{s}$  in fluid solutions at room temperature. (Sacksteder, L., Lee, M., Demas, J.N., and DeGraff, B.A. (1993) *J. Am. Chem. Soc.* 115, 8230-8238). Our novel Re(I) complex is a remarkable example of such a high quantum

25 yield long lifetime probe. It displays a lifetime over 10  $\mu\text{s}$  in air-equilibrated glycerol, and long lifetimes

when the lipid conjugate Re-PE is embedded in DPPG model vesicles, as shown in Table 1. Owing to its long lifetime, it is also extremely sensitive to oxygen quenching. There is a significant increase in  
5 intensity with the removal of oxygen from the solution, as shown in Figure 3. In methanol, in the absence of oxygen, a homogeneous intensity decay with a lifetime of 7248 ns was found. In the presence of dissolved oxygen, from equilibrium with air, the lifetime reduced  
10 to 538 ns (Figure 4). This result suggests that this complex may be used as an oxygen sensor under certain circumstances. The oxygen quenching, however, is much less efficient when the probe is bound to macromolecules, such as phospholipid vesicles, than  
15 when free in solvents (Figure 5). We attribute this to a shielding of the excited state from oxygen quenching by macromolecules. More importantly, this complex displays a lifetime of 2.54  $\mu$ s and a quantum yield of 0.13 in DPPG vesicles in aqueous solution at 22 °C,  
20 which indicates that this long-lived probe can be used in presence of dissolved oxygen and still display a long decay time and exhibit a high quantum yield.

We also studied the polarized emission of this complex in the absence of rotational diffusion  
25 (glycerol, -60°C). The excitation anisotropy spectrum is shown in Figure 2 which displays a maximum anisotropy near 0.3 from 390 nm to 450 nm. The anisotropy of this complex is also sensitive to solution viscosity, as shown in Figure 20. Figure 20  
30 is not meant to yield an exact relationship between the anisotropy and solution viscosity. For example, at the same temperature, the viscosity of a 100% glycerol solution is larger than that of a 60% glycerol:water

solution, and the anisotropy values demonstrate this behavior.

Rhenium (I) complexes are known to display dual emission, which can originate from either a metal-to-ligand charge transfer state or a ligand-centered state (LC). The MLCT states typically show an unstructured emission whereas the LC states often display a structural emission which is characteristic of ligand. The emission spectra in Figure 2 are unstructured, suggesting that under our experimental conditions the emission is from a pure MLCT state. The  $R(\lambda)$  values are flat across the excitation spectrum, which suggests that regardless of excitation wavelength, only one excited state parentage is created (Figure 21).

To further clarify the nature of the emission, and to characterize this complex for use as biophysical probe, we examined the emission anisotropy (Figure 22). The anisotropy is rather constant across the entire emission spectrum and displays a gradual decrease with increasing wavelength.

For use as a biomolecular probe, this complex was used to label the proteins bovine IgG and HSA, as well as the lipid PE. The lipid conjugate Re-PE was used to label the DPPG vesicles. The preliminary results demonstrate that this complex is conjugatable and that its water solubility is adequate for the usual labeling procedures used with the biomolecules. The typical frequency-domain intensity decays of DPPG vesicles labeled with Re-PE are shown in Figure 6. The decays were best fit using three exponential components, along with a scattering component. The recovered long lifetimes when bound to proteins and lipid model vesicles indicate that this complex might be used to

study protein and membrane hydrodynamics and measure rotational correlation times longer than 10  $\mu$ s.

Example 2:

*Fluorescence Polarization Immunoassays of High*

5 *Molecular Weight Analytes*

Human serum albumin (HSA), human immunoglobulin G (IgG), and monoclonal IgG specific for HSA (anti-HSA) from mouse ascites were obtained from Sigma Chemical Co. and were used without further purification. All  
10 other reagents and all solvents used were reagent grade. The synthesis of  $[\text{Re}(\text{bcp})(\text{CO})_3(4\text{-COOHPy})](\text{ClO}_4)$  is described in Example 1.

5 mg of N,N'-dicyclohexylcarbodiimide (DCC) and 3 mg of N-hydroxy-succinimide (NHS) were dissolved in  
15 0.15 mL of DMF with stirring.  $[\text{Re}(\text{bcp})(\text{CO})_3(4\text{-COOHPy})](\text{ClO}_4)$  (10 mg in 0.15 mL of DMF) was added, and the mixture was stirred for 20 hours. The formed precipitate was removed by filtration through a syringe filter, and the filtrate containing the activated Re-  
20 complex was used for labeling the substrates.

The protein HSA (10 mg) was labeled by adding a 15-fold molar excess of the activated Re-complex in 50  $\mu$ l of DMF to 1 mL of stirring protein solution (0.2 M carbonate buffer, pH 8.5), followed by a 5 hr  
25 incubation. The conjugate was purified by gel filtration chromatography on Sephadex G-25, using 0.1 M PBS, pH 7.0 as eluent. The dye:protein ratio of the Re-HSA conjugate was determined to be 2:1. The concentration of the protein was determined by the  
30 Coomassie Plus Protein Assay. The concentration of the Re(I) complex was determined by its absorbance at 400 nm, assuming the extinction coefficient was the same as

that of the free dye ( $\epsilon_{400} = 5040 \text{ M}^{-1}\text{cm}^{-1}$ ). (Guo, S.Q., Li, L., Castellano, F.N., Szmecinski, H., Lakowicz, J.R. *Anal. Biochem.* submitted). The equilibrium association constants of the bioconjugates were  
5 determined from luminescence anisotropy data as described in the literature. (Dandliker, W.B., Kelly, R.J., Dandliker, J., Farquhar, J., Levin, J. *Immunochemistry* 1973, 10, 219-227).

Uncorrected emission spectra were recorded on a  
10 SLM AB2 Spectrofluorimeter. The frequency-domain lifetime measurements were performed on an ISS K2 fluorimeter, using a high intensity Panasonic blue LED (light-emitting diode) configured to provide amplitude modulated light centered at 390 nm. (Guo, X.Q., Li,  
15 L., Castellano, F.N., Szmecinski, H., Lakowicz, J.R. *Anal. Biochem.* Submitted; Sipior, J., Carter, G.M., Lakowicz, J.R., Rao, G. *Rev. Sci. Instrum.* 1997, 68(7), 1-5). An Andover 500 nm long pass filter (500FH90-50S) was used to isolate the emission.

20 The frequency-domain intensity decay data were fit by a nonlinear least squares procedure, generally to a sum of three single-exponential decays. The intensity decays were described by Equation 9. Mean lifetimes were calculated using Equation 10.

25 The excitation anisotropy spectrum is defined by Equation 5, where  $I_{\parallel}$  and  $I_{\perp}$  are the emission intensities measured with vertically polarized excitation and the emission polarization parallel ( $I_{\parallel}$ ) or perpendicular ( $I_{\perp}$ ) to the excitation. The values of the polarized  
30 intensities were corrected for the transmission efficiency of the polarized components by the detection optics.

The molecular structure of  $[\text{Re}(\text{bcp})(\text{CO})_3(4\text{-COOHpy})]^+$  is shown in Figure 1. The absorption and emission spectra of  $[\text{Re}(\text{bcp})(\text{CO})_3(4\text{-COOHpy})]^+$  labeled to HSA are shown in Figure 23. The spectra are normalized to unity for comparative purposes. The absorption profile in the low-energy region (340-425 nm) and the more intense higher energy band at 290 nm are characteristic metal-to-ligand charge transfer and  $\pi - \pi^*$  transitions, respectively. The emission spectrum is broad and has a maximum near 550 nm. These photophysical characteristics are similar to that observed with the parent complex  $[\text{Re}(\text{bcp})(\text{CO})_3(\text{py})]^+$ , where py is pyridine. (Zipp, A.P., Sacksteder, L.A., Streich, J., Cook, A., Demas, J.N., DeGraff, B.A. *Inorg. Chem.* 1993, 32, 5629-5632). The large Stokes' shift of MLCT complexes in general can be exploited in biological media where multiple labeling of close proximity residues will not result in self-quenching processes.

$\text{O}_2$  quenching is commonplace from MLCT excited states of Re(I) complexes. (Guo, X.Q., Li, L., Castellano, F.N., Szmecinski, H., Lakowicz, J.R. *Anal. Biochem.* Submitted; Sacksteder, L.A., Zipp, A.P., Brown, E.A., Streich, J., Demas, J.N., DeGraff, B.A. *Inorg. Chem.* 1990, 29, 4335-4340; Zipp, A.P., Sacksteder, L.A., Streich, J., Cook, A., Demas, J.N., DeGraff, B.A. *Inorg. Chem.* 1993, 32, 5629-5632). In the case of  $[\text{Re}(\text{bcp})(\text{CO})_3(4\text{-COOHpy})]^+$ , the oxygen quenching is modest when the probe is bound to HSA in air-equilibrated aqueous solution. Compared to a deoxygenated buffer solution (1.0), the relative photoluminescence intensity of Re-HSA in air-equilibrated buffer solution is 0.69 (Figure 7).

We examined the steady-state excitation anisotropy spectrum of  $[\text{Re}(\text{bcp})(\text{CO})_3(4\text{-COOHPy})]^+$  in vitrified solution (glycerol,  $-60^\circ\text{C}$ ) where rotational diffusion does not occur during the excited state lifetime (Figure 23). This complex shows a maximum anisotropy near 0.3, whose values are constant from 390 nm to 450 nm.

Frequency-domain intensity decays of Re-HSA in air-equilibrated and argon-equilibrated 0.1 M PBS buffer solutions are shown in Figure 8. The analysis of the frequency-domain intensity decays are summarized in Table 2.

Table 2. Recovered intensity decays parameters of  $[\text{Re}(\text{bcp})(\text{CO})_3(4\text{-COOHPy})]^+$  conjugated to HSA.

15	Condition	$\tau_i (\mu\text{s})$	$\alpha_i$	Mean $\tau (\mu\text{s})$
	Re-HSA      Air	5.76	0.02	
		1.27	0.13	
		0.053	0.85	2.75
	Argon	6.23	0.03	
		1.39	0.11	
		0.051	0.87	3.44

The decays were best fit to a sum of three-exponential decay laws. The mean lifetimes are 2.75  $\mu\text{s}$  in air-equilibrated and 3.44  $\mu\text{s}$  in argon-equilibrated buffer solutions, respectively. The elimination of oxygen is therefore not required for use in fluorescence polarization immunoassays of high molecular weight analytes.

To evaluate the feasibility of using  
[Re(bcp)(CO)<sub>3</sub>(4-COOHPy)]' in a polarization immunoassay,  
Re-HSA was used as an antigen. We examined the changes  
in anisotropy of Re-labeled HSA in the presence of  
5 increasing amounts of anti-HSA. The polarization  
increased about four-fold from 0.023 to 0.108 which  
corresponds to anisotropy values ranging between 0.017  
to 0.075 (Figure 9). Similar results were obtained  
using two different batches of anti-HSA with antibody  
10 (Ab) concentrations ranging from 0 to 8 times that of  
Re-HSA (Ag). An association constant was calculated  
from the data in Figure 9 and found to be 3.3  $\mu\text{M}^{-1}$ . We  
used nonspecific human IgG as a control, and no  
detectable changes in polarization of Re-HSA were  
15 observed in that experiment (Figure 9).

A competitive assay for HSA utilizes labeled and  
unlabeled antigens which are allowed to simultaneously  
compete for the binding sites on the antibody. The  
simultaneous exposure of the labeled and unlabeled HSA  
20 to anti-HSA resulted in a constant anisotropy at all  
concentrations. This may reflect a higher affinity of  
anti-HSA for unlabeled HSA or the formation of  
aggregates around the labeled antigen. However,  
preincubation of the unlabeled HSA with anti-HSA for 30  
25 minutes, followed by the addition of the Re-labeled  
antigen, resulted in measurable changes in anisotropy.  
In this sequential assay, the anisotropy was found to  
decrease with increasing amounts of unlabeled HSA  
(Figure 24). The concentrations of Re-labeled HSA and  
30 anti-HSA were 2.5  $\mu\text{M}$  and 4.5  $\mu\text{M}$ , respectively. At high  
concentrations of unlabeled HSA, the anisotropy could  
not be reversed to the value for unbound Re-HSA  
( $r=0.017$ ,  $p=0.023$ ), which should be observed on total

replacement of Re-HSA with unlabeled HSA. This effect could be explained by non-specific binding of Re-HSA to other proteins present in the solution. However, the polarization of Re-HSA was not influenced by the presence of non-specific proteins in the IgG ascites fluid (Figure 9). Another reason for this behavior may be a result of a higher binding affinity for Re-HSA than for free HSA or possibly irreversible interactions between the Ab and Ag.

10        Example 3:

*Anisotropy Probe for Protein Hydrodynamics*

Human serum albumin (HSA), bovine immunoglobulin G (IgG), were obtained from Sigma Chemical Co. and were used without further purification. 2,9-dimethyl-4,7-diphenyl-1,10-phenanthroline (bcp), isonicotinic acid (4-COOHPy), AgClO<sub>4</sub>, NH<sub>4</sub>PF<sub>6</sub>, and Re(CO)<sub>5</sub>Cl were from Aldrich Chemical Co. and used as received. The other solvents used were of HPLC or spectroscopic reagent grade.

20        5 mg of N,N'-dicyclohexylcarbodiimide (DCC) and 3 mg of N-hydroxy-succinimide (NHS) were dissolved in 0.15 ml of DMF with stirring, 10 mg of the Re-complex in 0.15 ml of DMF was then added, and the mixture was stirred for a few hours. The formed precipitate was removed by filtration through a syringe filter, and the filtrate containing the active Re-complex was used for labeling the substrates.

25        The proteins HSA and IgG (10 mg of protein) were labeled by adding a 15-fold molar excess of the activated Re-complex in 50 µl of DMF to 1 ml of stirred protein solution (0.2 M carbonate buffer, pH 8.5), followed by a 5 h incubation. The conjugates were purified by gel filtration chromatography on Sephadex

G-25 or G-50, using 0.1 M  $\text{Na}_2\text{HPO}_4$  - 0.1 M  $\text{NaH}_2\text{PO}_4$  (0.1 M PBS) buffer, pH 7.0, as eluent. The dye:protein ratios of Re-HSA and Re-IgG conjugates were determined to be 2:1 and 3:1, respectively. The concentration of protein was determined by the Coomassie Plus Protein Assay. The concentration of Re (I) complex was determined by its absorbance at 400 nm, assuming the extinction coefficient ( $\epsilon_{400 \text{ nm}} = 5040 \text{ M}^{-1} \text{ cm}^{-1}$ ) was the same as that of the free dye.

Fluorescence intensity and anisotropy decays were measured by time-correlated single photon counting (TCSPC). (Birch, D.J.S., and Imhof, R.E., In *Topics in Fluorescence Spectroscopy, Vol. 1: Techniques*, Lakowicz, J.R., Ed., Plenum, New York, (1991) pp. 1-45). The light source was the output of a Pridine 1 dye laser, cavity dumped at 0.19 MHz and frequency doubled to 380 nm. For TCSPC measurements the emission was isolated using a long pass filter transmitting above 520 nm. The detector was a Hamamatau R2809 red-sensitive microchannel plate PMT.

The time-domain intensity data were fitted by the usual procedures of nonlinear least squares and were fitted to single and multi-exponential decay laws. The intensity decays were described by Equation 9. The fitting was carried out by using software from IBH Software (Edinburgh, Scotland).

The time-resolved anisotropy decays were obtained by measuring the time dependent decays of the vertically ( $I(t)$ ) and horizontally ( $I(t)$ ) polarized components of the emission

$$r(t) = \frac{I_{\parallel}(t) - I_{\perp}(t)}{I_{\parallel}(t) + 2I_{\perp}(t)} \quad (12)$$

These data were fitted to a single and double correlation time model, using the IBH software,

$$r(t) = \sum_i r_{0i} e^{-t/\theta_i} \quad (13)$$

5 where  $r_{0i}$  are the amplitudes and  $\theta_i$  are the rotational correlation times.

The excitation anisotropy spectra were collected as usual, with the anisotropy defined by

$$10 \quad r(\lambda) = \frac{I_{\parallel}(\lambda) - I_{\perp}(\lambda)}{I_{\parallel}(\lambda) + 2I_{\perp}(\lambda)} \quad (14)$$

Steady-state fluorescence data were obtained using a spectrofluorometer from SLM Instruments, with magic-angle polarizer conditions and a Hamamatsu R-928 detector. The emission spectra are uncorrected for the wavelength dependence of the detection system.

15 The molecular structure of  $[\text{Re}(\text{bcp})(\text{CO})_3(4\text{-COOHpy})]^+$  is shown in Figure 1. The absorption and excitation spectra of the Re-complex in  $\text{CH}_3\text{OH}$  are shown in Figure 25. The absorption spectra of the ligands in  $\text{CH}_3\text{OH}$  are also shown for comparison. The spectra are normalized to unity to facilitate comparison. The absorption spectral maxima of the low-energy absorption band around 340 ~ 450 nm and the more intense higher energy absorption at 298 nm are the characteristic

20 metal-to-ligand charge transfer (MLCT) and  $\pi\text{-}\pi^*$  absorption, respectively. The emission originates from MLCT states, with two maximal excitation bands at ~345 nm and ~390 nm, respectively. It is important to note that a complex with absorption near 380 nm can be

25 excited with the UV output of a light emitting diode.

30

The emission spectra of Re-complex in  $\text{CHCl}_3$ ,  $\text{CH}_3\text{OH}$  and Re-HSA and Re-IgG conjugates are shown in Figure 26. The large Stokes' shift of the Re-complex and its protein conjugates (~100 nm) makes it a good candidate for energy transfer studies and other biophysical studies as there is no possibility for self quenching. This Re-complex displays high quantum yields (>0.5) in fluid solutions at room temperature. The influence of oxygen is modest when it is bound to macromolecules.

To be useful as an anisotropy probe for study of macromolecular dynamics, the Re-complex needs to display polarized emission. We studied the polarized emission in the absence of rotational diffusion. The excitation anisotropy spectra of  $[\text{Re}(\text{bcp})(\text{CO})_3(4\text{-COOHPy})]^+$  and its protein conjugates, Re-HSA and Re-IgG, are shown in Figure 27. In the absence of rotational motion, this complex shows maximal anisotropies near 0.3 and these high anisotropies are broadly available from 390 nm to 450 nm. The steady-state anisotropy of  $[\text{Re}(\text{bcp})(\text{CO})_3(4\text{-COOHPy})]^+$  and its conjugates were measured as a function of temperatures and/or viscosities (Figure 28). The solvent used for this study was 60% glycerol/40% buffer (v/v), which formed a highly viscous solution at -60 °C. The results show that the anisotropy values are nearly the same for the free dye and the Re-protein conjugates at -60 °C. The steady-state anisotropy of the free  $[\text{Re}(\text{bcp})(\text{CO})_3(4\text{-COOHPy})]^+$  decreases rapidly as the temperatures are changed from low temperature, -60 °C towards high temperature, 20 °C, whereas the anisotropies of Re-HSA and Re-IgG decrease more slowly with temperature, and remain adequate for measurement at room temperature. These results demonstrate that the anisotropies are sensitive to rotational motion, and the anisotropy of the Re-protein

conjugates is lost by fast motions of the probe in addition to rotational motion of the proteins. Importantly, the anisotropies of the labeled protein are always larger than that of free dye, indicating that protein hydrodynamics contributes to the anisotropy.

To further demonstrate that the anisotropy depends on rotational diffusion we examined the time-dependent anisotropy of free  $[\text{Re}(\text{bcp})(\text{CO})_3(4\text{-COOHpy})]^+$  in 100% glycerol and 60% glycerol/40% buffer (v/v) at -60 °C and 20 °C. At 20 °C, the anisotropy decays rapidly with a correlation time near 4 ns in 60% glycerol/40% buffer (v/v), whereas the anisotropy decays more slowly with a correlation time of 118 ns in 100% glycerol. At -60 °C, the anisotropy decays much more slowly with a correlation time 82  $\mu\text{s}$  in 100% glycerol (Figure 29).

Time-resolved anisotropy decays of Re-protein conjugates are shown in Figure 30. Analysis of these anisotropy decays are summarized in Table 3.

Table 3. Time-resolved Intensity Decay ( $\tau$ ), Rotational Correlation Times ( $\theta$ ) of free  $[\text{Re}(\text{bcp})(\text{CO})_3(4\text{-COOHPy})]^+$  and its protein conjugates.

	Sample	$\tau_i$ (ns)	$f_i^*$	$\chi_R^2$	$\theta_i$ (ns)	$r_{10}$	$\chi_R^2$
5	ReCOOH in 60% glycerol	1478	1	1.2	4	0.0713	0.97
	RE-HSA in 60% glycerol	7	0.0024		12	0.168	
		79	0.021		457	0.0789	1.0
10		1402	0.98	1.1			
	Re-HSA in 30% glycerol	10	0.0089		12	0.157	
		952	0.93		282	0.104	1.0
		1068	0.063	1.1			
	Re-HSA in buffer	18	0.02		16	0.143	
		781	0.84		164	0.0788	1.2
		143	0.14	1.2			
	Re-IgG in 60% glycerol	14	0.0014		6	0.0614	
		1986	0.97		379	0.0384	2.0
15		153	0.025	1.0			
	Re-IgG in buffer	21	0.0088		10	0.0800	
		606	0.86		271	0.0595	1.2
		134	0.13	1.1			

$$* f_i = \frac{\alpha_i \tau_i}{\sum_i \alpha_i \tau_i}$$

Free  $[\text{Re}(\text{bcp})(\text{CO})_3(4\text{-COOHPy})]^+$  anisotropy decay are fitted to single exponential anisotropy decay model, whereas the anisotropy decays of Re-labeled protein are fitted to a double exponential decay model, reflecting

a fast motion of the probe and a slower protein rotational diffusion. In addition, the anisotropy decay of labeled IgG appears to be somewhat more complex than labeled HSA, suggesting that independent domain motions of IgG contribute to the anisotropy decay. The results demonstrate that the anisotropy decays are dependent on protein rotational diffusion and inter-domain dynamics. The anisotropy decays are slowed by adding glycerol as a result of the slower protein rotational diffusion.

10        Example 4:

*Red Fluorescent Dyes for Biophysics and for Sensors*

      All chemicals and solvents were purchased from Aldrich Chemical Co. and used without further purification. The ligand tppz was purchased from GF  
15        Chemicals and recrystallized before use, and ligands ttpy (Spahni, W. And Galzaferri, G. *Helv. Chim. Acta.*, 1984, 67, 450; Constable, E.C. and Thomson, A.M., *J. Chem. Soc., Dalton Trans.* (1994) 2947) and mcbpy (Strouse, G.F., Schoonover, J.R., Duesing, R., Boyed,  
20        S., Jones, W.E. Jr., Meyer, T.J., *Inorg. Chem.*, 1995, 34, 473) were synthesized using reported procedures.

      All absorbance spectra were recorded on a Hewlett Packard diode array (HP 8453) spectrophotometer. All emission spectra were recorded on a SLM AB2  
25        spectrophotometer. The excitation anisotropy spectra were measured at -55 °C in 9:1, glycerol:methanol by weight, using a SLM 800 spectrophotometer. Excitation anisotropy spectra were collected as usual, with the anisotropy defined by Equation 5, where  $I_{\parallel}$  and  $I_{\perp}$  are  
30        the intensities measured with vertically polarized excitation and the emission polarization parallel ( $\parallel$ ) or perpendicular ( $\perp$ ) to the excitation. The values of

the polarized intensities were corrected for the transmission efficiency for the polarized components by the detection optics. The reported emission spectra are corrected for variation in the detector efficiency with observation wavelength.

Fluorescence intensity decays were measured with frequency-domain instrumentation (Laczko, G. Grycznski, I., Wiczak, W., Malak, H. and Lakowicz, J.R., *Rev. Sci. Instrum.* 1990, 61, 2331). The excitation wavelength was 488 nm using an air cool argon laser supplied by Omnicrome Inc. The frequency-domain data were used to determine the intensity decay law using multiexponential model

$$I(t) = \sum_{i=1}^n \alpha_i e^{-t/\tau_i} \quad (15)$$

where  $\alpha_i$  are the preexponential factors,  $\tau_i$  are decay times, and  $n$  is the number of exponential components. The mean decay time is given by

$$\bar{\tau} = \alpha_i \tau_i^2 / \sum \alpha_j \tau_j \quad (16)$$

#### *Synthesis of Complexes*

All of these complexes were synthesized as  $\text{PF}_6$  salts by following two different methods which depend on the ligand used. Method A describes the synthesis of complexes using tridentate ligands (L-L-L) generally ttpy, tpy, tppz and triphos. Method B describes the synthesis of complexes using bidentate ligands (L-L) which consist of mcbpy, phen and aphen ligands. Both methods are modifications of reported methods

- (Kober, E.M., Marshall, J.L., Dressick, W.J., Sullivan, B.H., Casper, J.V. and Mayer, T.J. *Inorg. Chem.*, (1984) 24, 2755; Brewer, R.G., Jensen, G.E. and Brewer, K.J. *Inorg. Chem.*, (1994) 33, 124; Kober, E.M., Marshall, J.L., Dressick, W.J., Sullivan, B.H., Casper, J.V. and Meyer, T.J. *J. Am. Chem. Soc.*, (1980) 102, 7385; Arana, C.R. and Abruna, H.O. *Inorg. Chem.* (1993) 32, 194; Sauvage, J.P., Collin, J.H., Chambron, J.C., Guillerez, S. Coudret, C., Balzani V., Bariegalletti, F., Cola, L.D., and Flamigni, L., *Chem. Rev.* (1994) 94, 993).

*Synthesis of  $[\text{Os}(\text{L-L-L})_3]^{2+}$ , with Tridentate Ligands (Method A)*

- In this typical synthesis, one equivalent of  $\text{OsCl}_3$  and one equivalent of tridentate ligands, L-L-L, (where L-L-L is either ttpy, tppz or triphos) was heated at reflux in 100 ml of ethanol, and a black precipitate of  $\text{Os}(\text{L-L-L})\text{Cl}_3$  forms after three hours of heating. This precipitate was filtered after cooling and washed with water and ethanol. This is the starting material for the desired compounds,  $[\text{Os}(\text{L-L-L})_3]^{2+}$ . Equal molar ratios of  $\text{Os}(\text{L-L-L})\text{Cl}_3$  and the appropriate ligand were further heated at reflux in 20 ml of ethylene glycol for one hour, which produces a brown solution. After cooling, about 100 ml of a saturated solution of ammonium hexafluorophosphate in water was added. After a few minutes, a dark brown-black precipitate formed. This precipitate was separated out by vacuum filtration and dried. All these compounds were recrystallized after dissolving them in acetonitrile and crystallizing them by using an excess amount of ether. They were chromatographed on neutral alumina using a 5:2 toluene:acetonitrile mixture.

*Synthesis of  $[\text{Os}(\text{L-L})_3]^{2+}$ , with Bidentate Ligands  
(Method B)*

The starting material,  $\text{Os}(\text{L-L})_2\text{Cl}_2$ , for all these compounds was synthesized by mixing one equivalent of  
5  $(\text{NH}_4)_2\text{OsCl}_6$  and two equivalents of bidentate ligands L-L, (where L-L are either mcbpy, phen or aphen). This reaction mixture was heated at reflux for about one hour in 50 ml of ethylene glycol. A dark brown precipitate was obtained which was filtered and washed  
10 with water and ethanol. For making  $[\text{Os}(\text{L-L})_3]^{2+}$  complexes, equal molar ratios of  $\text{Os}(\text{L-L})_2\text{Cl}_2$  and the appropriate ligand were further heated at reflux in 20 ml of ethylene glycol for about six hours, which produced a greenish brown solution. After cooling this  
15 reaction mixture, about 100 ml of a saturated solution of ammonium hexafluorophosphate in water was added, and a dark green precipitate separated out. The precipitate was filtered by vacuum filtration and dried. These dried compounds were recrystallized by  
20 dissolving them in acetonitrile and crystallizing them out by adding a large amount of ether. It was chromatographed on neutral alumina using a 2:1 toluene:acetonitrile mixture.

*Electronic Absorption Spectroscopy*

25 The electronic spectra of these osmium complexes in acetonitrile are shown in Figure 11 and summarized in Table 4.

Table 4. Spectral properties of the red osmium probes

Probes <sup>a</sup>	$\lambda_{\max}^{\text{abs}}$	$\lambda_{\max}^{\text{em}}$	$\tau$ (ns) <sup>c</sup>	$\Phi^c$	$r_o^d$
	(nm) <sup>c</sup>	(nm) <sup>b</sup>			
[Os(ttpy) <sub>2</sub> ] <sup>2+</sup>	500	735	220	0.02	0.15
5 [Os(3,2,1)] <sup>2+</sup>	550	640	130	0.015	--
[Os(tpy)(triphos)] <sup>2+</sup>	470	710	230	--	0.35
[Os(phen) <sub>2</sub> (aphen)] <sup>2+</sup>	485	700	195	0.02	0.02
[Os(tppz) <sub>2</sub> ] <sup>2+</sup>	480	740	175	0.016	0.18

<sup>a</sup> All are PF<sub>6</sub> salts; <sup>b</sup> measured in acetonitrile;

10 <sup>c</sup> measured in deoxygenated acetonitrile; <sup>d</sup> measured in 9:1 glycerol:methanol mixture at -55°C.

The ultraviolet region of the tridentate ligands are similar to each other and are dominated by the  $\pi$ - $\pi^*$  transitions from the ligand. The visible region of the electronic spectra of tridentate complexes contains  
 15 intense bands centered between 450-500 nm. These transitions represent the lowest lying <sup>1</sup>MLCT, which is Os(d $\pi$ )-L-L-L( $\pi^*$ ) in nature for all these complexes. Due to the high degree of spin-orbit coupling in osmium,  
 20 transitions that are formally spin forbidden exhibit enhanced intensity. (650 nm). These MLCT transitions appear as tails on the low energy end of the more intense <sup>1</sup>MLCT transition.

*Emission Spectroscopy, Quantum Yields and Excited State Lifetimes*

The emission maxima, quantum yields, and lifetimes are outlined in Table 4. All these complexes emit at 700-750 nm at room temperature, Figure 12, when they are excited at 480 to 550 nm. Similar trends are seen in the emission and absorption energies of all these complexes. All of these complexes have excited-state lifetimes around 200 ns. The lifetime of the [Os(tppz)]<sup>2+</sup> complex was found to be 175 ns. The quantum yields of all these complexes are around 2 percent which is typical for all these red emitting osmium(II) complexes (Kober, E.M., Marshall, J.L., Dressick, W.J., Sullivan, B.H., Casper, J.V. and Mayer, T.J. *Inorg. Chem.*, (1984) 24, 2755; Sauvage, J.P., Collin, J.H., Chambron, J.C., Guillerez, S. Coudret, C., Balzani, V., Barigelletti, F., Cola, L.D., and Flamigni, L., *Chem. Rev.* (1994) 94, 993).

*Fundamental Anisotropy ( $r_0$ ).*

Anisotropy of these complexes are measured in 9:1 (glycerol:methanol by weight) at -55 °C and summarized in Table 4, and shown in Figure 13. The trend of the anisotropy depends on the structure of the molecules. More asymmetric molecules show higher anisotropies. The complex [Os(tpy)(triphos)]<sup>2+</sup> is the most asymmetric molecule, and therefore shows a high anisotropy value (0.35).

Since many modifications, variations, and changes in detail may be made to the described embodiments, it is intended that all matter in the foregoing description and shown in the accompanying drawings be

interpreted as illustrative and not in a limiting sense.

CLAIMS

1. A method of conducting an assay of a sample containing an analyte of interest, comprising the steps of:

5       forming a mixture so as to bring a metal-ligand complex into interactive proximity with said sample containing said analyte of interest;       irradiating said mixture with electromagnetic light energy so as to cause emission of light indicative of said analyte of interest; and  
10       measuring the emitted light and utilizing the measurement of the emitted light so as to measure the analyte of interest.

2. A method as defined by claim 1, wherein said  
15       assay is used to characterize a high molecular weight antigen.

3. A method as defined by claim 2, wherein said analyte of interest is human serum albumin.

4. A method as defined by claim 1, wherein said  
20       assay is used to characterize protein hydrodynamics.

5. A method as defined by claim 4, wherein said analyte of interest is human serum albumin and bovine immunoglobulin G.

6. A method as defined by claim 1,  
25       wherein said assay is used to characterize a sample lipid; and       wherein said metal-ligand complex is coupled to a lipid so as to form a lipid-probe complex.

7. A method as defined by claim 1, wherein said assay is used for oxygen sensing.

8. A method as defined by claim 1,  
wherein said assay is used to quantify said  
5 analyte of interest;  
wherein prior to said forming step, a first  
binding partner and a second binding partner are  
added to said sample, wherein said first binding  
partner competes with the analyte for binding to  
10 said second binding partner, wherein one of said  
first and second binding partner is labeled with a  
metal-ligand complex and the other is labeled with  
a photoluminescent energy transfer acceptor,  
wherein the metal-ligand complex and  
15 photoluminescent energy transfer acceptor are  
chosen such that when the first binding partner  
binds to the second binding partner, the metal-  
ligand complex and the photoluminescent energy  
transfer acceptor are brought into interactive  
20 proximity, producing a detectable change in  
luminescence.

9. A method as defined by claim 8,  
wherein subsequent to said measuring step,  
25 binding of the first binding partner to the second  
binding partner is quantified; and  
wherein said binding is quantified by a  
method from the group consisting of intensity,  
lifetime, and polarization, thereby quantifying  
30 the analyte.

10. A method as defined by claim 1, wherein  
fluorescence lifetime is measured.

11. A method as defined by claim 1, wherein said metal-ligand complex is coupled to said analyte of interest.

12. A method as defined by claim 1, wherein said metal-ligand complex is selected from the group consisting of Ru(II), Os(II), and Re(I).

13. A method as defined by claim 12, wherein said metal-ligand complex is selected from the group consisting of mono, bis, and tri(heteroleptic) complexes of Ru(II) and Os(II) and carbon monoxide diimine complexes of Re(I).

14. A method as defined by claim 1, wherein said metal-ligand complex is selected from the group consisting of  $[\text{Re}(\text{bcp})(\text{CO})_3(4\text{-COOHPy})]^+$ ,  $[\text{Os}(\text{phen})_2(\text{aphen})]^{2+}$ ,  $[\text{Os}(\text{tpy})(\text{triphos})]^{2+}$ ,  $[\text{Os}(\text{tppz})_2]^{2+}$ , and  $[\text{Os}(\text{tppy})_2]^{2+}$ .

15. A method as defined by claim 1, wherein said ligand is selected from the group consisting of ligands based on diimine, phosphine, arsine, pyridine, substituted pyridines, carbon monoxide, carbonyl, and any combination thereof.

16. A method as defined by claim 15, wherein said ligand is substituted with a functional group that can be directly conjugated to macromolecules selected from the group consisting of amine reactive N-hydroxysuccinimide, isothiocyanate, sulfonyl chloride containing ligands, sulfhydryl reactive iodoacetamide, and maleimide containing ligands.

17. A method as defined by claim 1,  
wherein said electromagnetic light energy is  
linearly polarized light energy; and  
wherein polarization of the emitted light is  
5 measured.

18. A method as defined by claim 17, wherein said  
linearly polarized light energy has a wavelength of  
about 400.

19. A method as defined by claim 17, wherein said  
10 linearly polarized high energy has a wavelength from  
280 to 1100 nm.

20. A metal-ligand complex of the formula  
 $[\text{Re}(\text{bcp})(\text{CO})_3(4\text{-COOHPy})]^+$ .

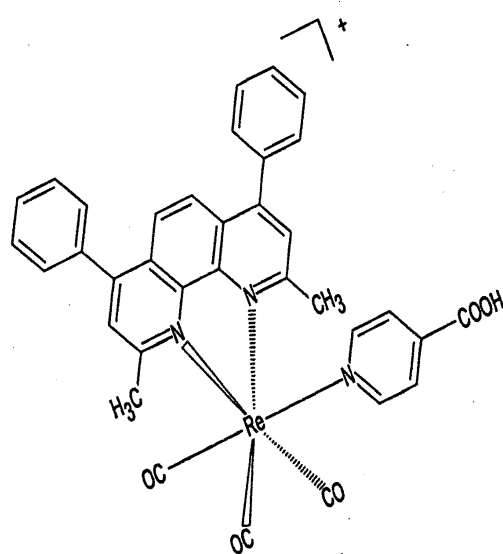


FIG. 1

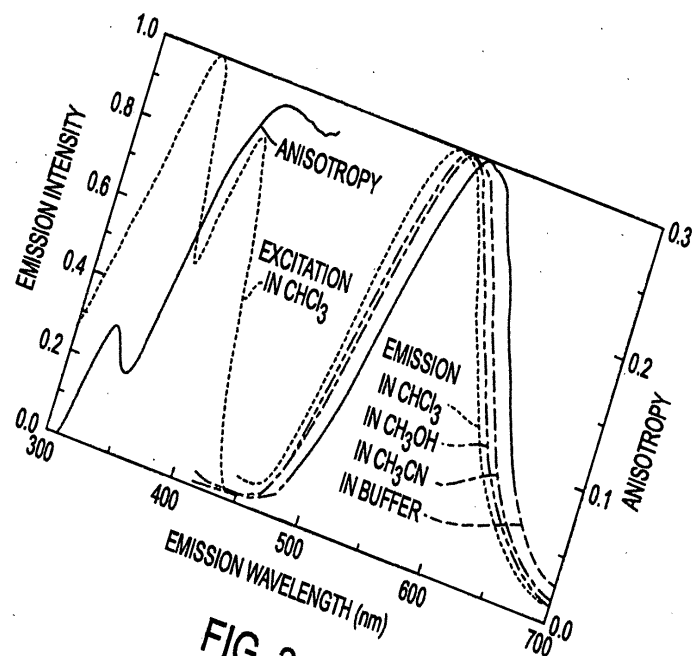


FIG. 2

3/29

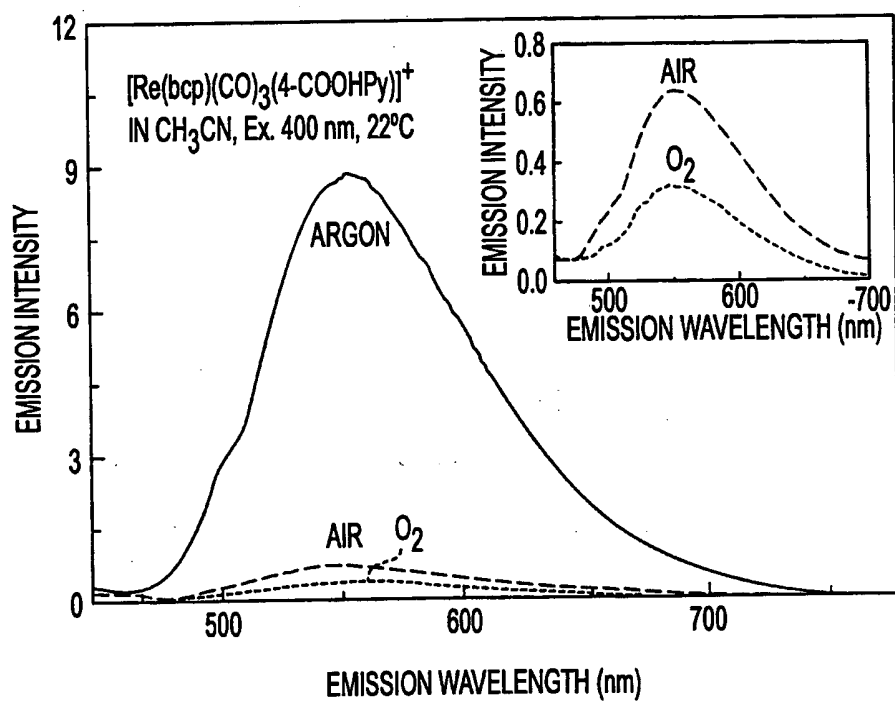


FIG. 3

4/29

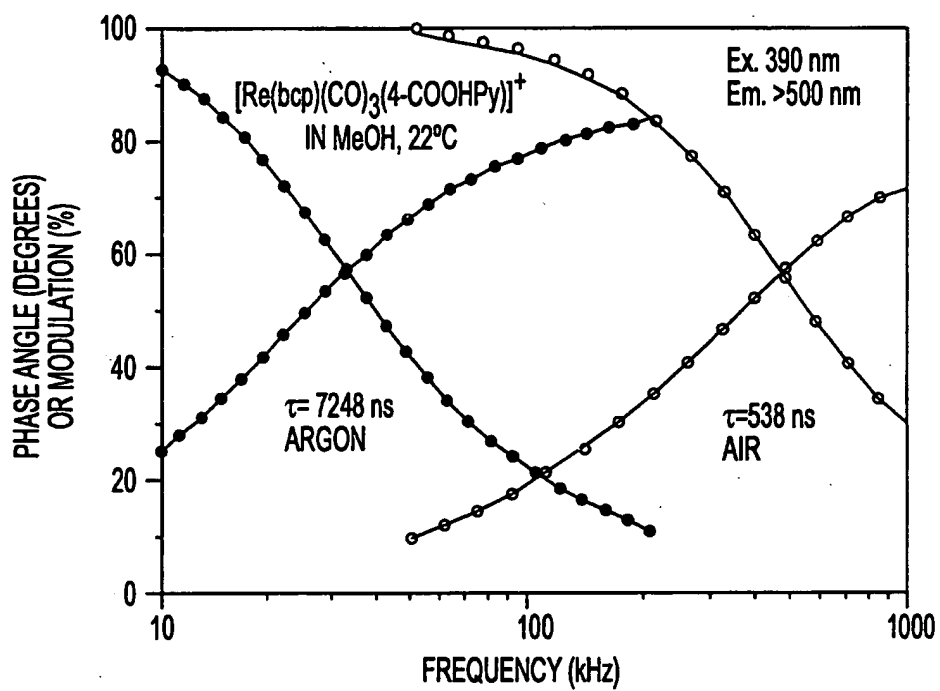


FIG. 4

5/29

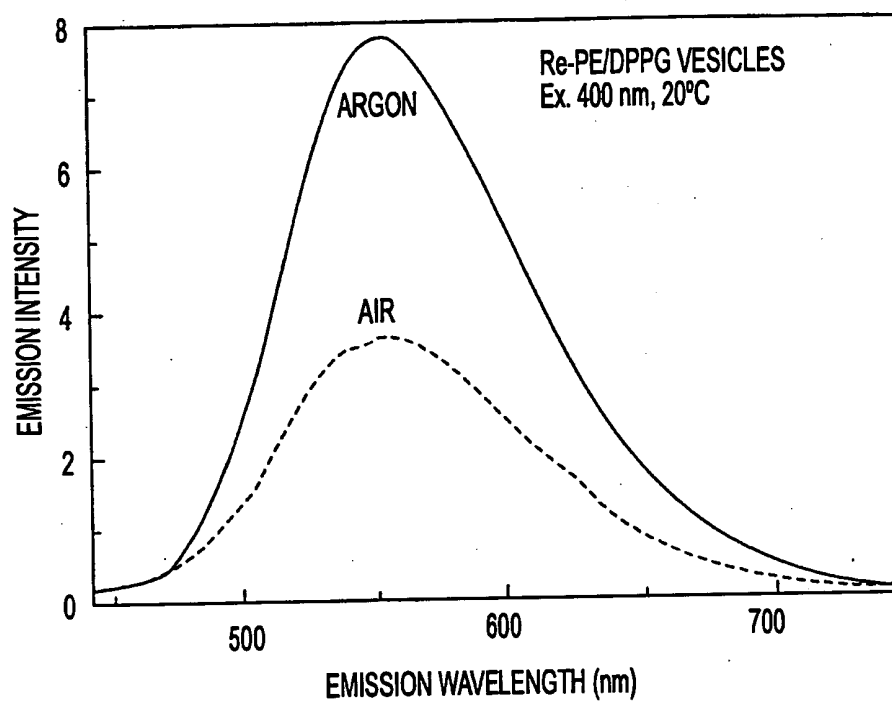


FIG. 5

6/29

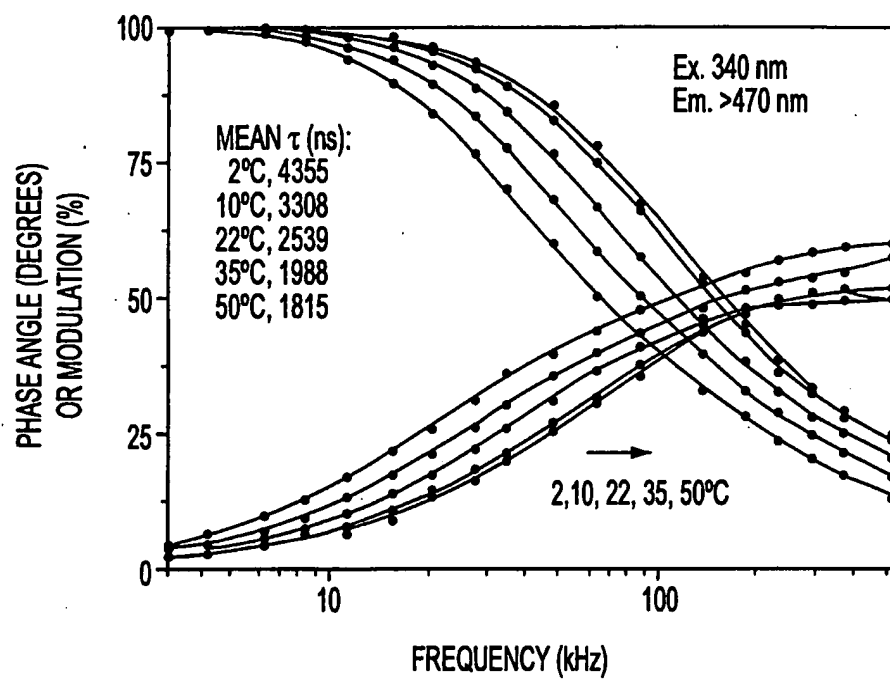


FIG. 6

7/29

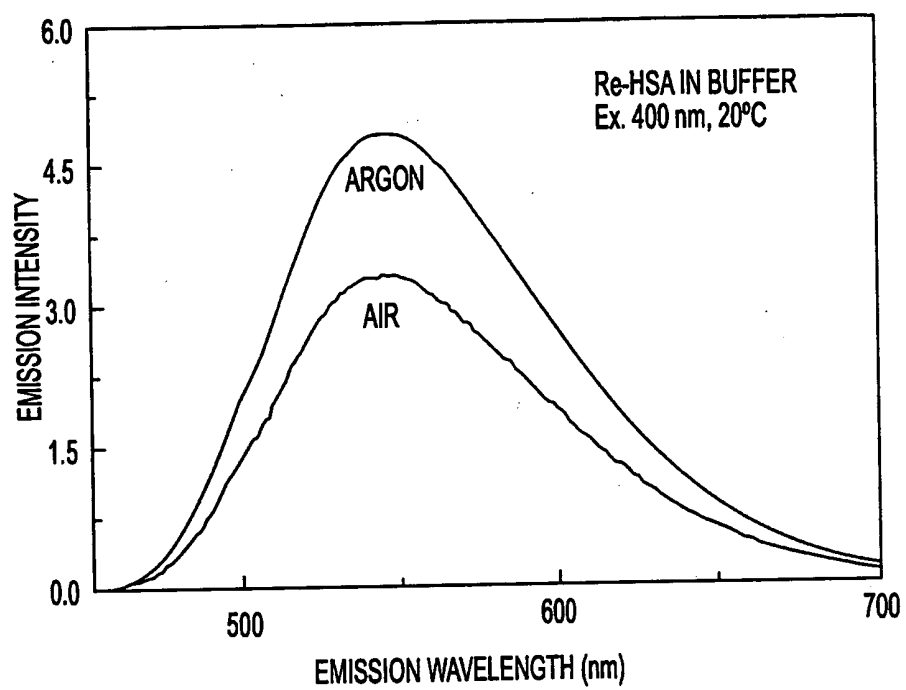


FIG. 7

8/29

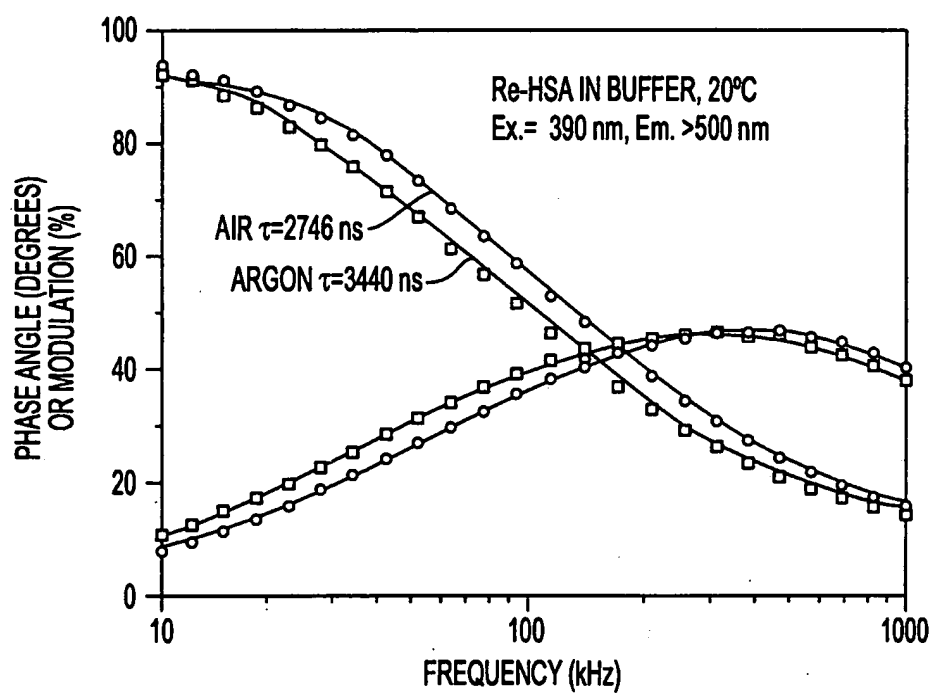


FIG. 8

9/29

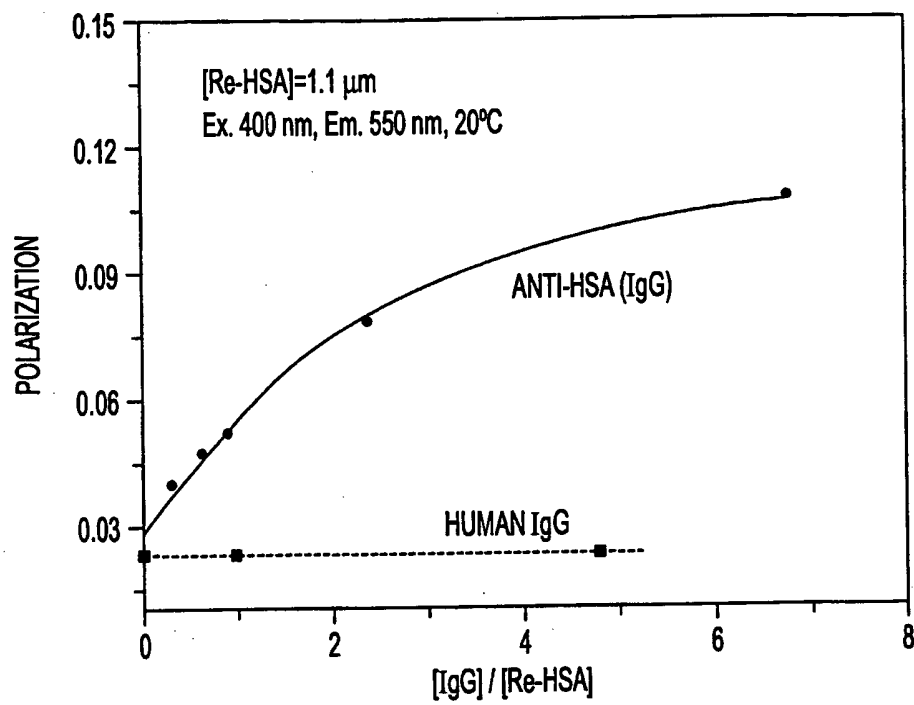


FIG. 9

10/29

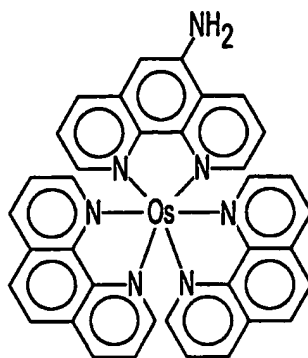


FIG. 10A

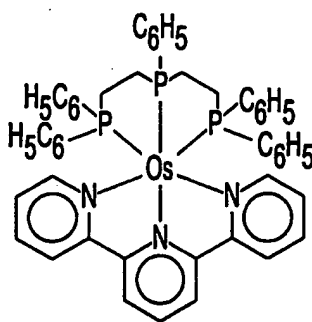


FIG. 10B

11/29

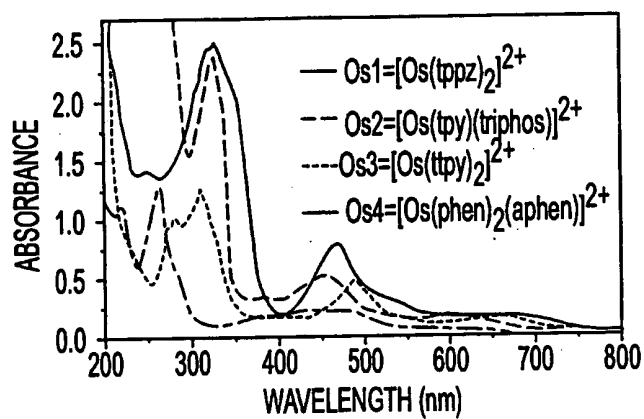


FIG. 11

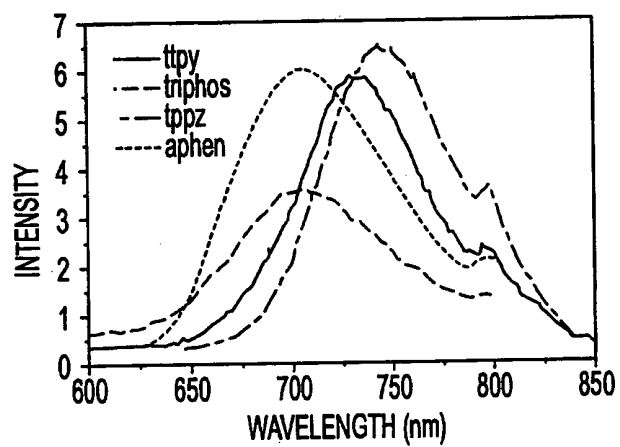


FIG. 12

12/29

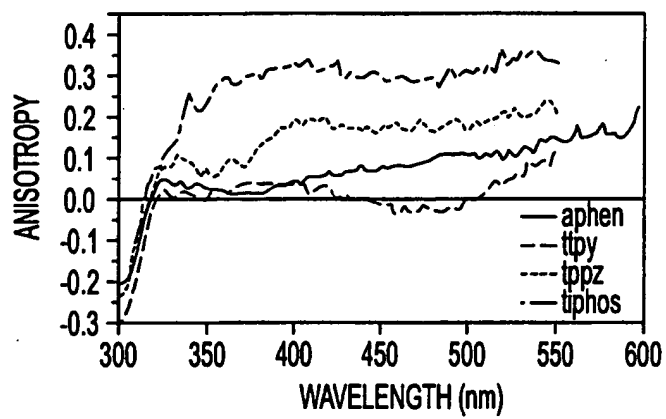


FIG. 13

13/29

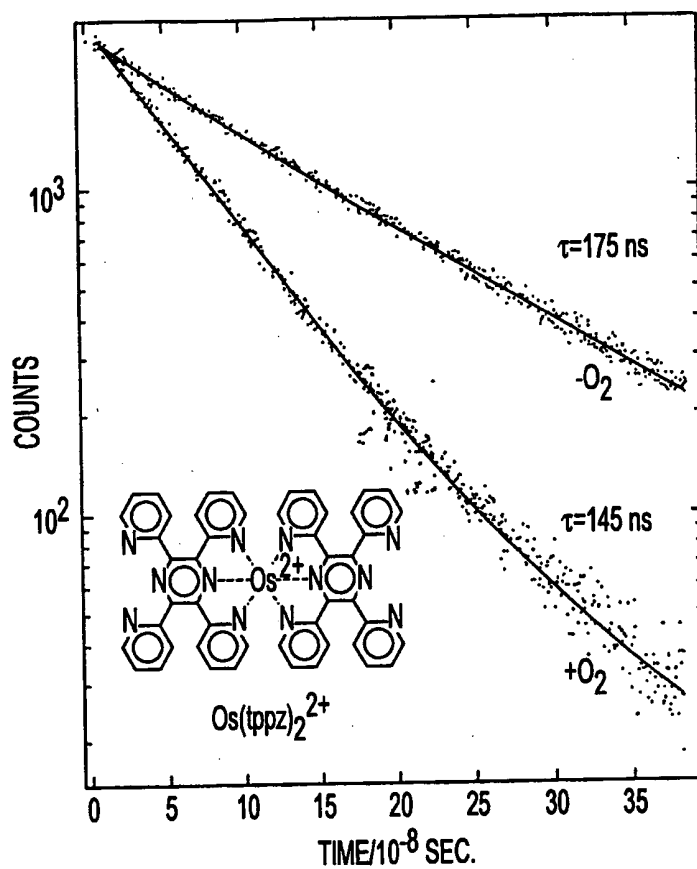


FIG. 14

14/29

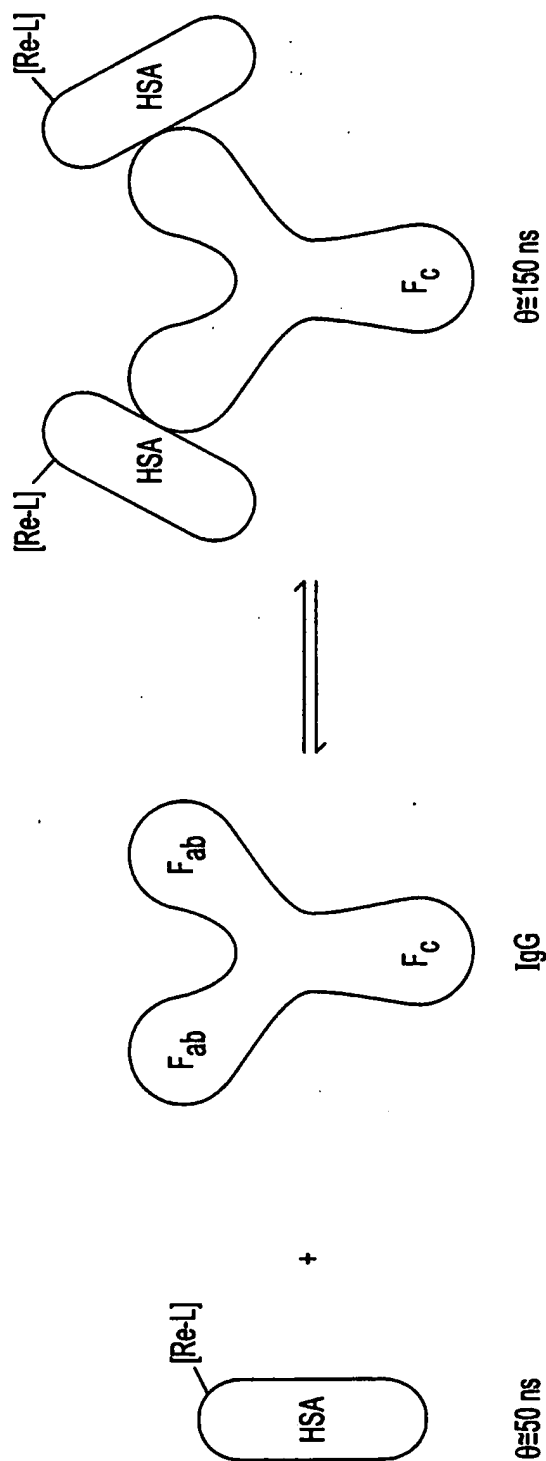


FIG. 15

15/29

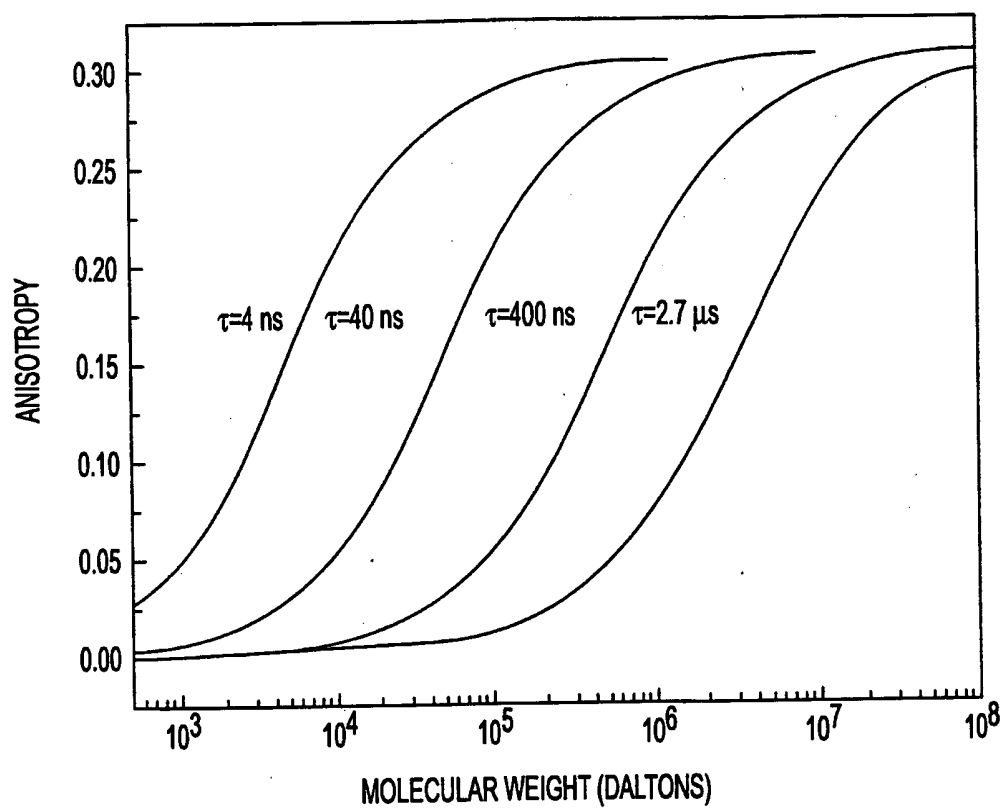
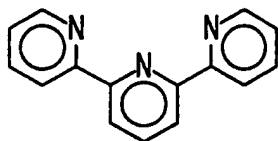


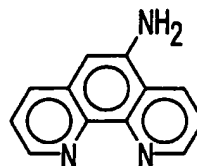
FIG. 16

16/29



2,2':6,2''-terpyridine (tpy,3)

FIG. 17A



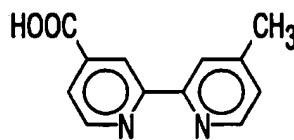
5-amino-phenanthroline (aphen)

FIG. 17B



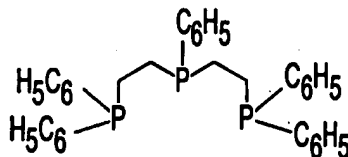
Pyridine (py,1)

FIG. 17C



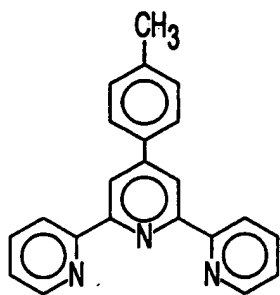
4-methyl,2,2'-bipyridine-4'-carboxylic acid (mcbpy,2)

FIG. 17D



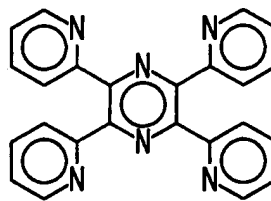
Bis(2-diphenylphosphinoethyl)phenyl phosphine (triphos)

FIG. 17E



4-tolyl, 2,2':6,2''-terpyridine (ttpy)

FIG. 17F



2,3,5,6-tetrakis(2-pyridyl)pyrazine (tppz)

FIG. 17G

17/29

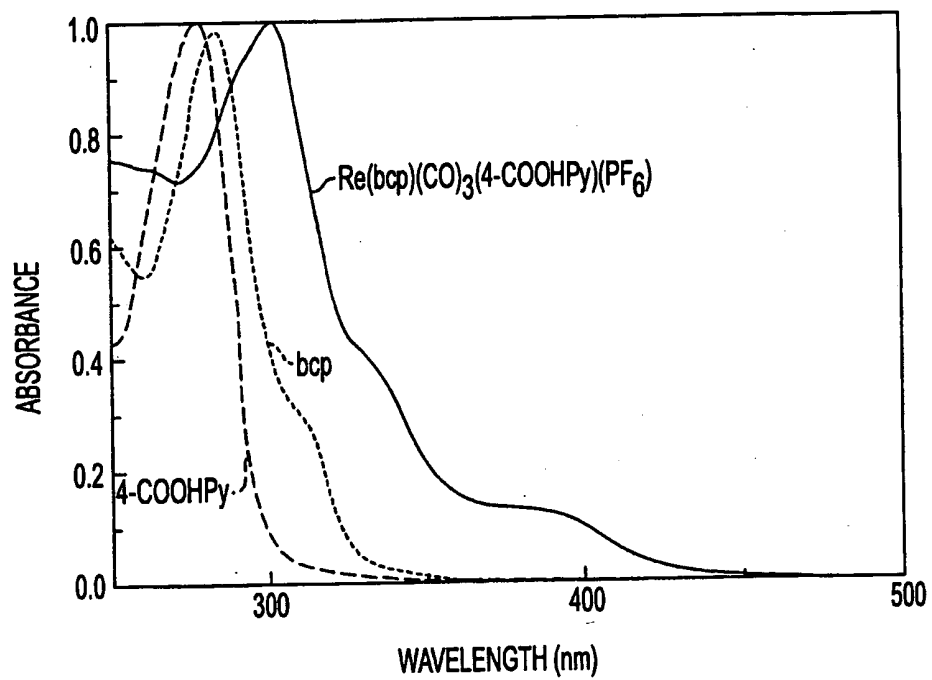


FIG. 18

18/29

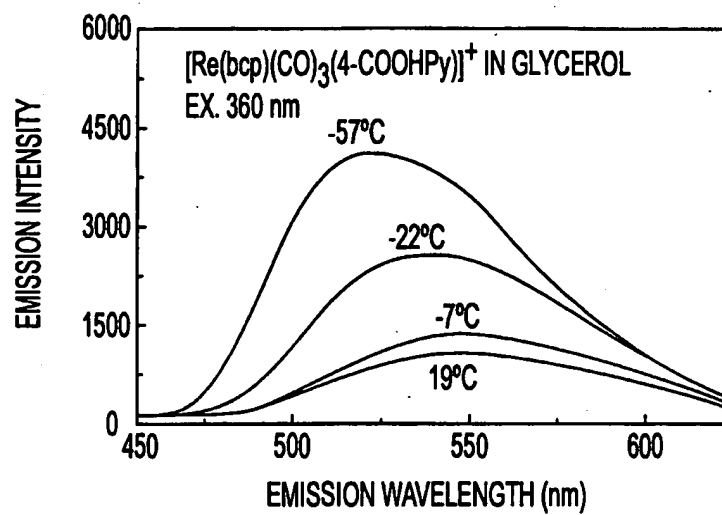


FIG. 19A

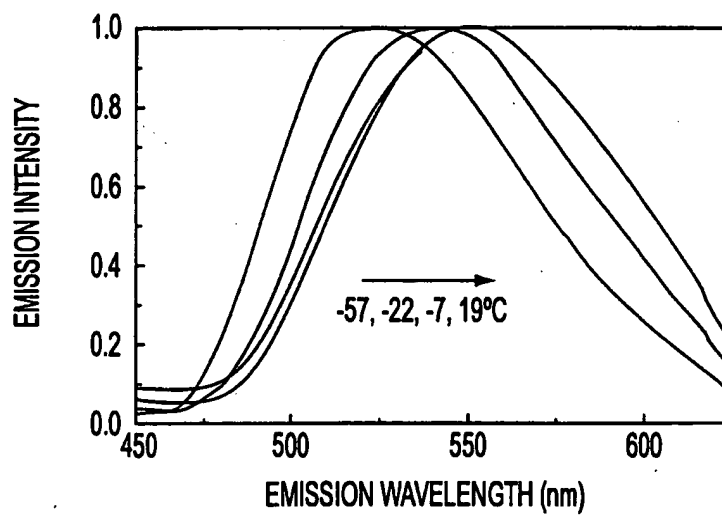


FIG. 19B

19/29

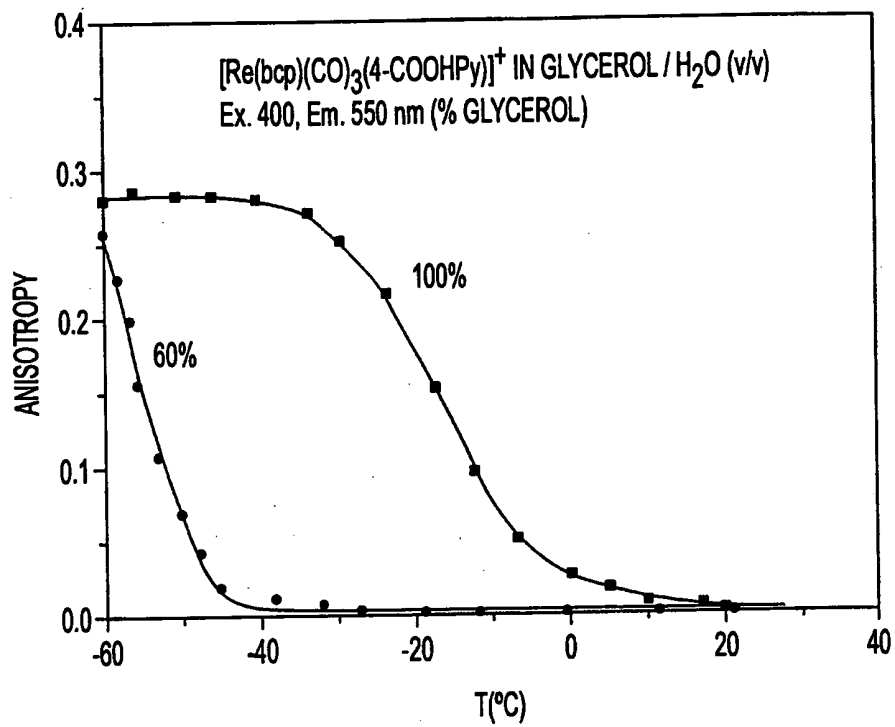


FIG. 20

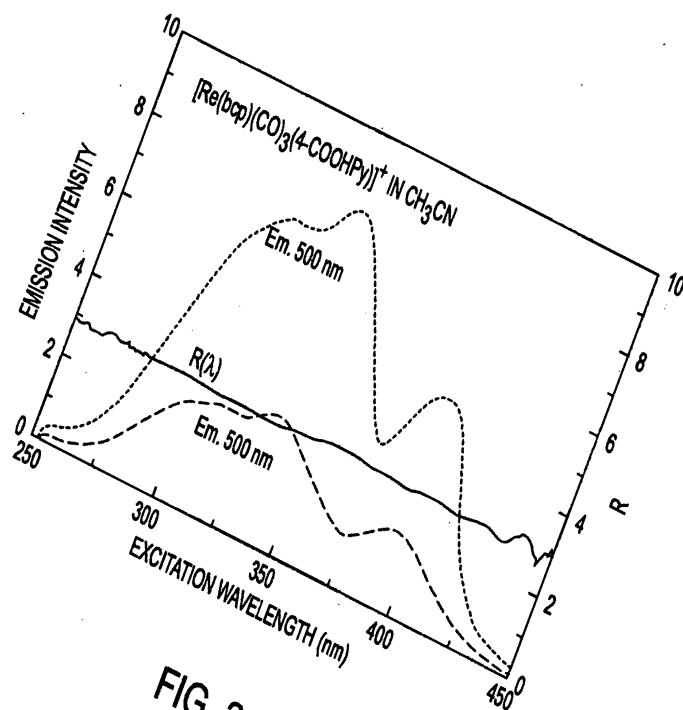


FIG. 21

21/29

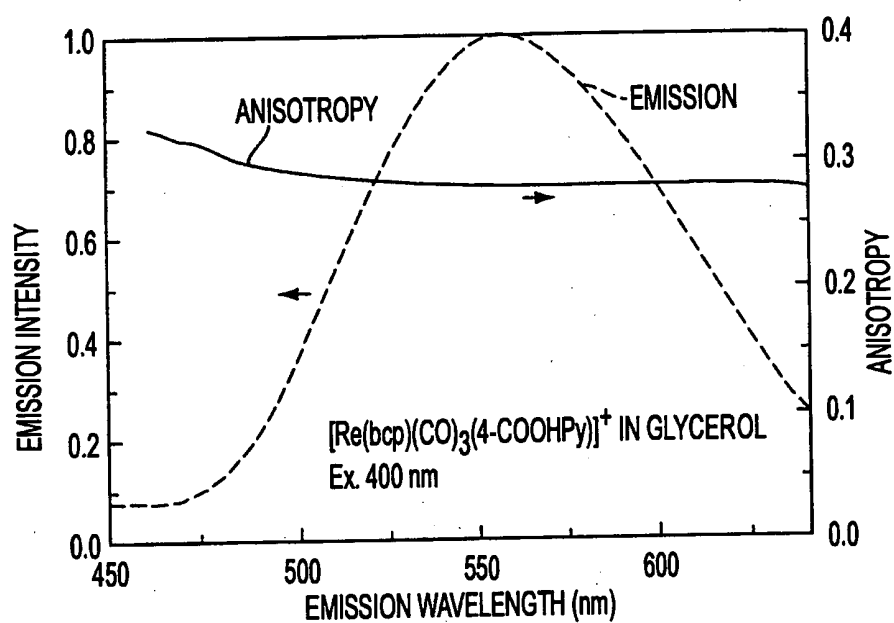


FIG. 22

22/29

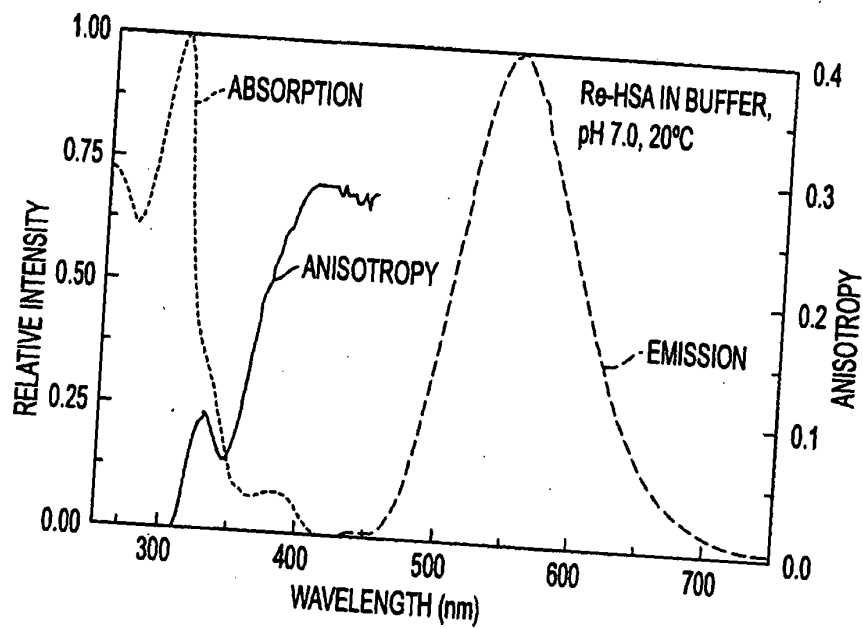


FIG. 23

23/29

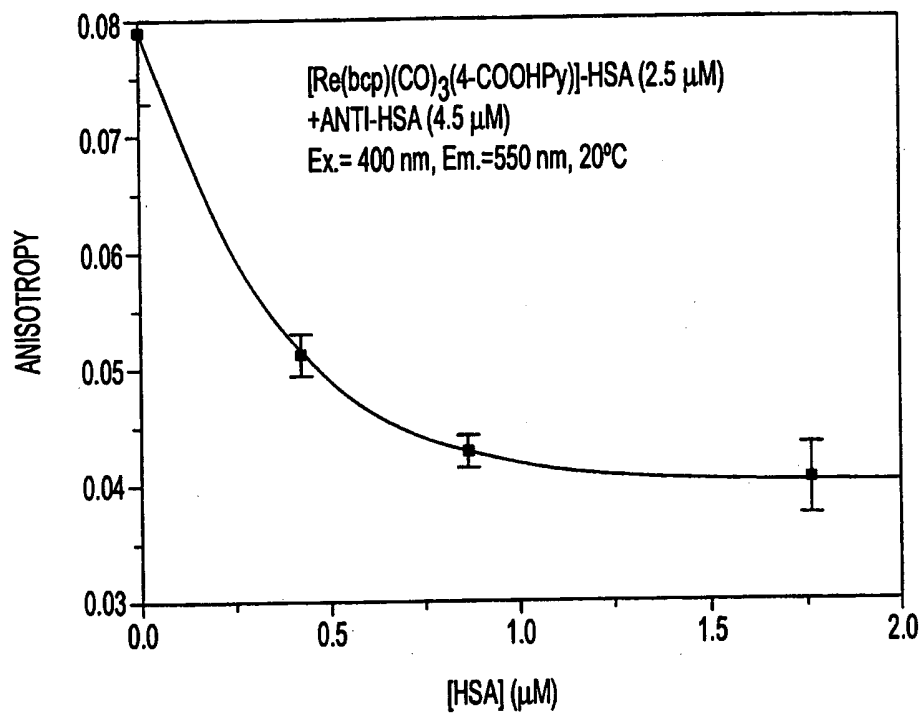


FIG. 24

24/29

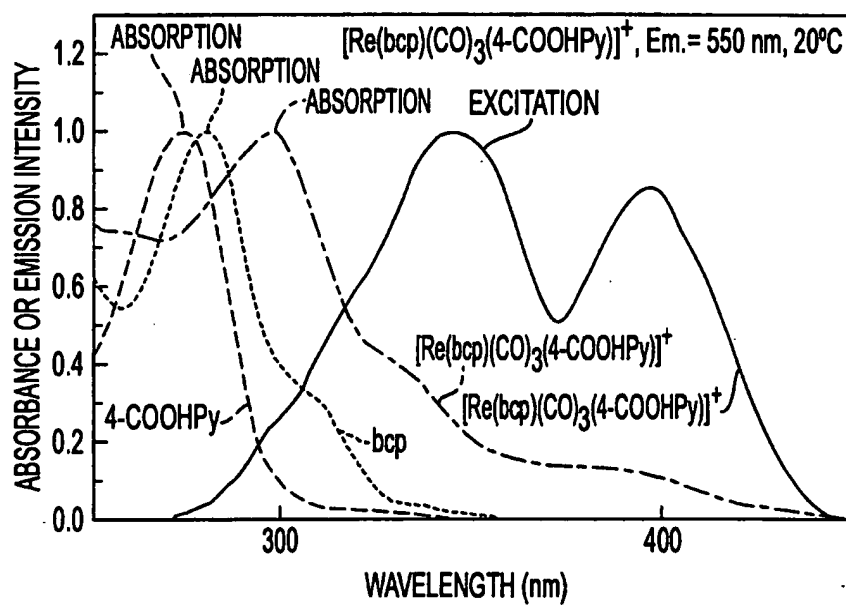


FIG. 25

25/29

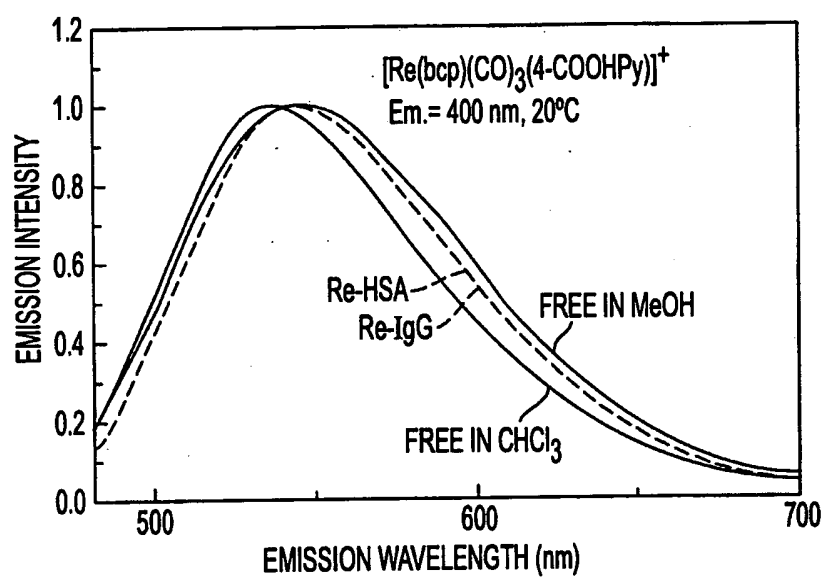


FIG. 26

26/29

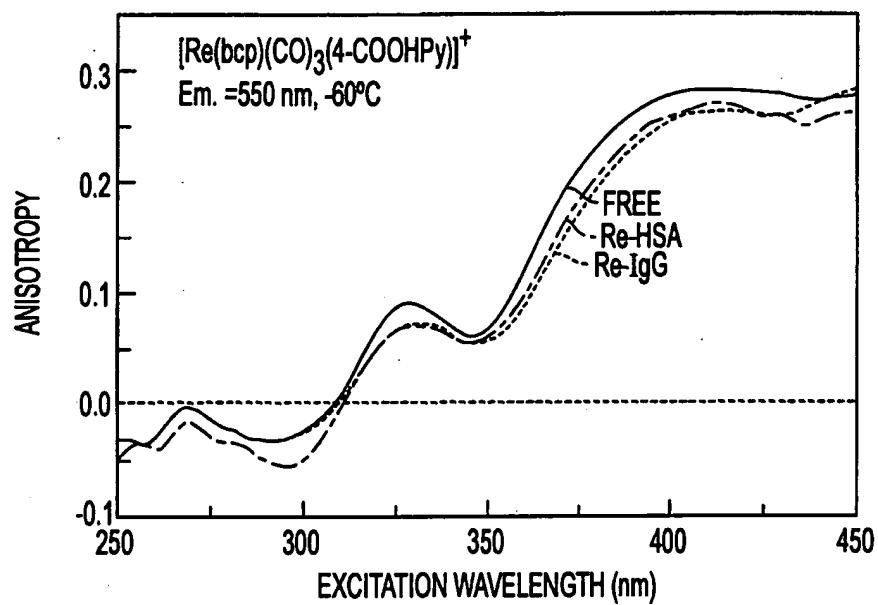


FIG. 27

27/29

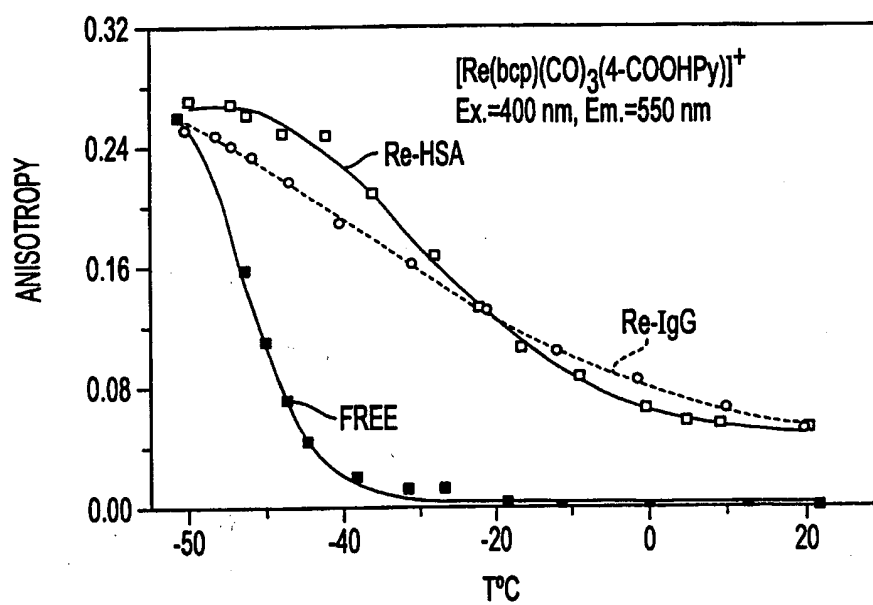


FIG. 28

28/29

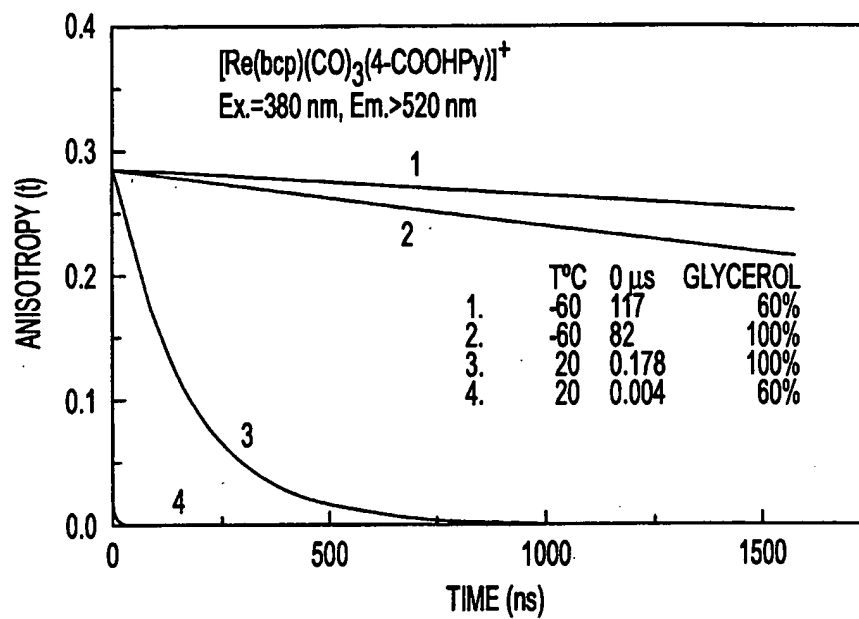


FIG. 29

29/29

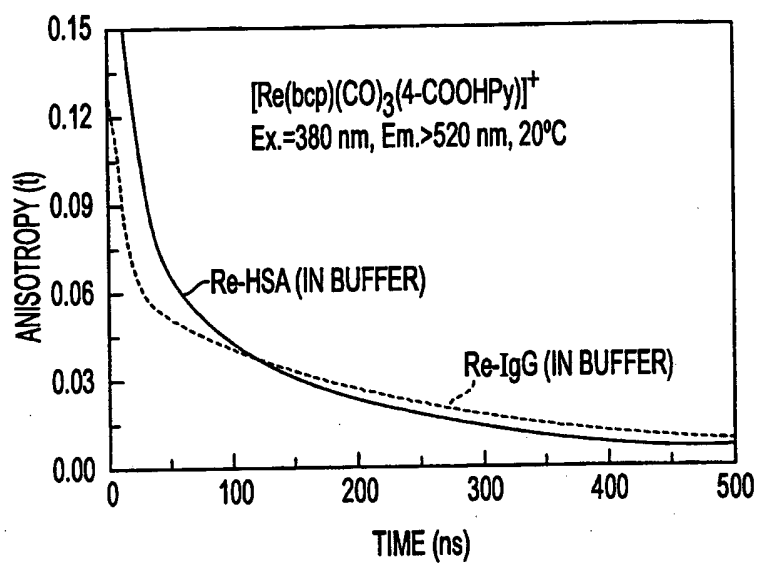


FIG. 30A

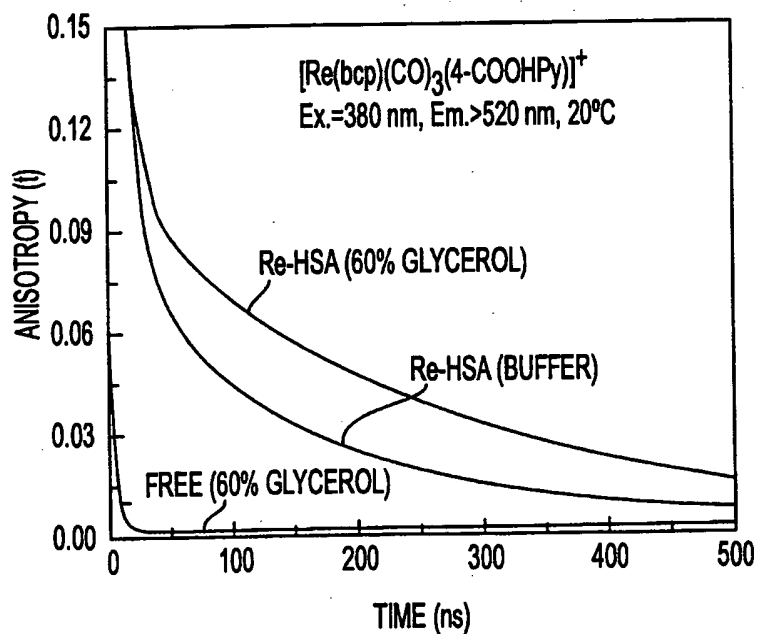


FIG. 30B

## INTERNATIONAL SEARCH REPORT

 International application No.  
PCT/US99/00774

## A. CLASSIFICATION OF SUBJECT MATTER

IPC(6) : G01N 33/533

US CL : 436/537, 536, 518, 546, 172; 422/82.07, 82.08, 82.09

According to International Patent Classification (IPC) or to both national classification and IPC

## B. FIELDS SEARCHED

Minimum documentation searched (classification system followed by classification symbols)

U.S. : 436/537, 536, 518, 546, 172; 422/82.07, 82.08, 82.09

Documentation searched other than minimum documentation to the extent that such documents are included in the fields searched

Electronic data base consulted during the international search (name of data base and, where practicable, search terms used)

APS, WPIDS

## C. DOCUMENTS CONSIDERED TO BE RELEVANT

Category*	Citation of document, with indication, where appropriate, of the relevant passages	Relevant to claim No.
Y	US 5,246,867 A (LAKOWICZ et al) 21 September 1993, see entire document.	1-20
Y	US 5,281,825 A (BERNDT et al) 25 January 1994, see entire document.	1-20
Y	US 5,624,847 A (LAKOWICZ et al) 29 April 1997, see entire document.	1-20
Y	US 5,628,310 A (RAO et al) 13 May 1997, see entire document.	1-20
Y	US 5,631,169 A (LAKOWICZ et al) 20 May 1997, see entire document.	1-20
Y	US 5,648,269 A (LAKOWICZ et al) 15 July 1997, see entire document.	1-20

☒ Further documents are listed in the continuation of Box C.
 ☐ See patent family annex.

* Special categories of cited documents:	*T* later document published after the international filing date or priority date and not in conflict with the application but cited to understand the principle or theory underlying the invention
*A* document defining the general state of the art which is not considered to be of particular relevance	*X* document of particular relevance; the claimed invention cannot be considered novel or cannot be considered to involve an inventive step when the document is taken alone
*B* earlier document published on or after the international filing date	*Y* document of particular relevance; the claimed invention cannot be considered to involve an inventive step when the document is combined with one or more other such documents, such combination being obvious to a person skilled in the art
*L* document which may throw doubts on priority claim(s) or which is cited to establish the publication date of another citation or other special reason (as specified)	*A* document member of the same patent family
*O* document referring to an oral disclosure, use, exhibition or other means	
*P* document published prior to the international filing date but later than the priority date claimed	

Date of the actual completion of the international search

12 APRIL 1999

Date of mailing of the international search report

14 MAY 1999

 Name and mailing address of the ISA/US  
Commissioner of Patents and Trademarks  
Box PCT  
Washington, D.C. 20231

Facsimile No. (703) 305-3230

Authorized officer

BAO-THUY L. NGUYEN

Telephone No. (703) 308-0196

 JOYCE BRIDGERS  
PARALEGAL SPECIALIST  
CHEMICAL MATRIX

# INTERNATIONAL SEARCH REPORT

International application No.  
PCT/US99/00774

C (Continuation). DOCUMENTS CONSIDERED TO BE RELEVANT		
Category*	Citation of document, with indication, where appropriate, of the relevant passages	Relevant to claim No.
Y	US 5,660,991 A (LAKOWICZ et al) 26 August 1997, see entire document.	1-20
Y,P	US 5,759,767 A (LAKOWICZ et al) 02 June 1998, see entire document.	1-20
Y,P	US 5,780,319 A (MAXFIELD WILSON et al) 14 July 1998, see entire document.	1-20